Annu. Rev. Biochem. 2000. 69:531–69

RECEPTOR BINDING AND MEMBRANE FUSION IN VIRUS ENTRY: The Influenza Hemagglutinin

John J. Skehel[1] and Don C. Wiley[2]
[1]*National Institute for Medical Research, London NW7 1AA, England*
[2]*Department of Molecular and Cellular Biology, Howard Hughes Medical Institute, Harvard University, Cambridge, Massachusetts 02138;*
e-mail: dcwadmin@crystal.harvard.edu

Key Words antigenic variation, sialic acid, viral glycoprotein, glycoprotein conformations, binding-site evolution

■ **Abstract** Hemagglutinin (HA) is the receptor-binding and membrane fusion glycoprotein of influenza virus and the target for infectivity-neutralizing antibodies. The structures of three conformations of the ectodomain of the 1968 Hong Kong influenza virus HA have been determined by X-ray crystallography: the single-chain precursor, HA0; the metastable neutral-pH conformation found on virus, and the fusion pH-induced conformation. These structures provide a framework for designing and interpreting the results of experiments on the activity of HA in receptor binding, the generation of emerging and reemerging epidemics, and membrane fusion during viral entry.

CONTENTS

Structures of HA in complex with sialic acid receptor analogs, together with binding experiments, provide details of these low-affinity interactions in terms of the sialic acid substituents recognized and the HA residues involved in recognition. Neutralizing antibody-binding sites surround the receptor-binding pocket on the membrane-distal surface of HA, and the structures of the complexes between neutralizing monoclonal Fabs and HA indicate possible neutralization mechanisms. Cleavage of the biosynthetic precursor HA0 at a prominent loop in its structure primes HA for subsequent activation of membrane fusion at endosomal pH (Figure 1). Priming involves insertion of the fusion peptide into a charged pocket in the precursor; activation requires its extrusion towards the fusion target membrane, as the N terminus of a newly formed trimeric coiled coil, and repositioning of the C-terminal membrane anchor near the fusion peptide at the same end of a rod-shaped molecule. Comparison of this new HA conformation, which has been formed for membrane fusion, with the structures determined for other virus fusion glycoproteins suggests that these molecules are all in the fusion-activated conformation and that the juxtaposition of the membrane anchor and fusion peptide, a recurring feature, is involved in the fusion mechanism. Extension of these comparisons to the soluble N-ethyl-maleimide-sensitive factor attachment protein receptor (SNARE) protein complex of vesicle fusion allows a similar conclusion.

RECEPTOR BINDING AND THE EVOLUTION OF RECEPTOR SPECIFICITY

The Receptor-Binding Site

Terminal sialic acids of glycoproteins and glycolipids are the cellular receptors for influenza virus (1, 2). They bind in a shallow depression at the top of the HA molecule, which is composed of residues conserved in all subtypes of influenza, throughout antigenic variation (3–6). A molecular model for bound sialic acid, which is based on 3-Å-resolution X-ray studies of complexes with sialyllactose

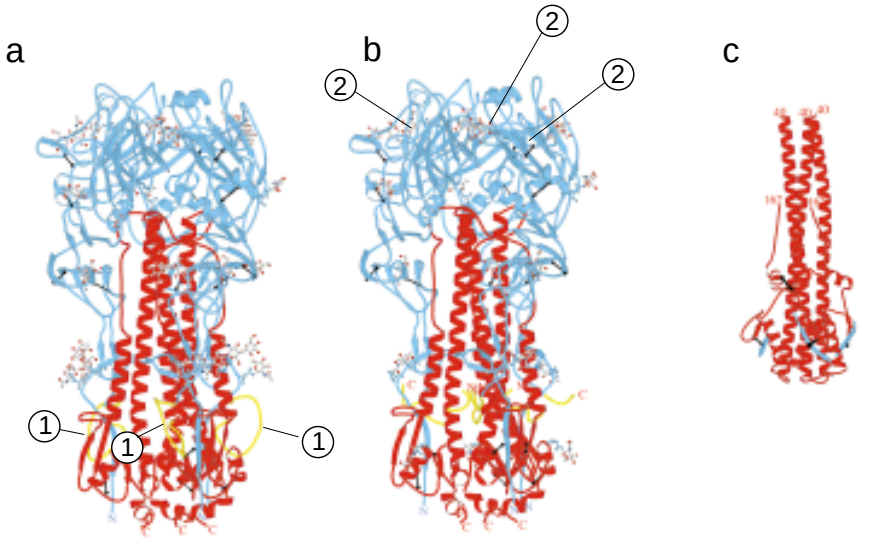

Figure 1 Three conformations of the hemagglutinin trimer. (*a*) Uncleaved precursor R329Q HA0 (82). *Circled 1* marks cleavage sites, residues 323 of HA1 to 12 of HA2 sites, and adjacent cavities in each monomer. Oligosaccharides are shown as *balls and sticks*; oligosaccharide at Asn-22 of HA1 is labeled as 22. (*b*) Cleaved BHA (3). Receptor-binding sites marked with *circled 2* (4). (*c*) Low-pH-induced conformation of thermolysin-solubilized TBHA2 (104); HA2, *shaded*; HA1, *unshaded*. Disulfide bonds are *black lines*. Figure prepared with MOLSCRIPT (202).

(4), was confirmed by crystal studies of complexes with other receptor analogs (6, 7), including a number of sialylated oligosaccharides (8). Irrespective of the receptor analog in these complexes, the structure and orientation of sialic acid are essentially identical; one side of the pyranose ring faces the base of the site, and the axial carboxylate, the acetamido nitrogen, and the 8- and 9-hydroxyl groups face into the site and form hydrogen bonds with conserved side-chain or main-chain polar atoms (Figure 2*a*). Specifically, conserved serine 136 forms a hydrogen bond with the carboxylate, which is also hydrogen bonded to the amide of peptide bond 137; histidine 183 and glutamic acid 190 form hydrogen bonds with the 9-hydroxyl group, and tyrosine 98 forms hydrogen bonds with the 8-hydroxyl group. The 5-acetamido nitrogen forms a hydrogen bond with the carbonyl of peptide bond 135, and the methyl group of this substituent is in van der Waals contact with the six-membered ring of tryptophan 153. The 7-hydroxyl group and acetamido carbonyl hydrogen bond to each other and form van der Waals contacts with leucine 194. By comparison, the 4-hydroxyl group projects out of the site and appears not to participate in binding. Consistent with these structural data, results from direct NMR binding studies of modified sialic acids to HA (7, 9, 10) and to viruses (11) and from competitive hemadsorption assays with viruses (12) also indicate the

(*a*)

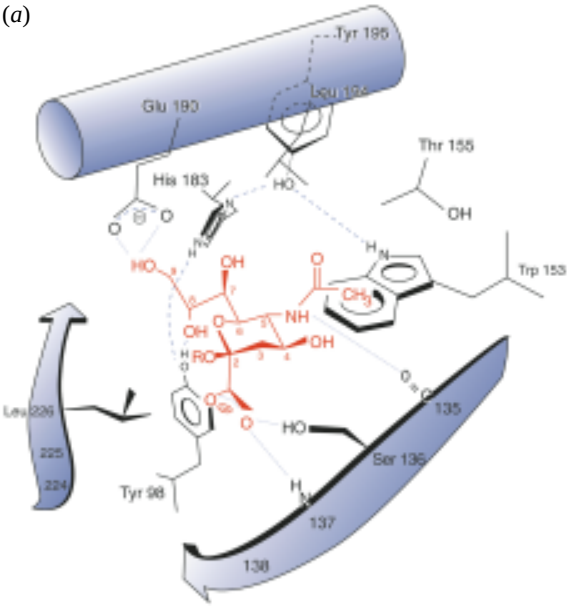

RBC Binding	
HA	% WT
WT	100
HA 225 G → R	136
HA 228 S → G	112
HA$_1$190 E → A	125
HA$_1$136 S → T	45
HA$_1$136 S → A	30
HA$_1$225 G → D	53
HA$_1$195 Y → F	36
HA$_1$226 L → P	42
HA$_1$ 98 Y → F	5
HA$_1$ 194 L → A	3
HA$_1$183 H → A	not expressed
HA$_1$183 H → F	12
HA$_1$153 W → A	not expressed
HA$_1$153 W → F	39

(*b*)

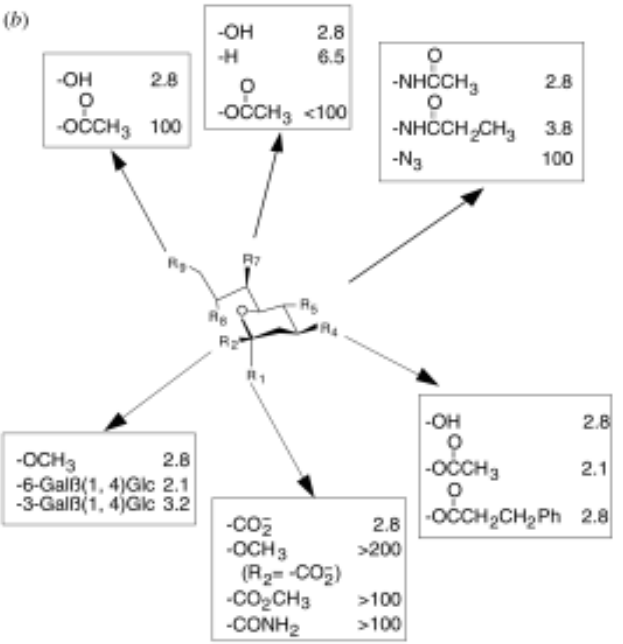

importance for binding of the axial carboxylate, the 7- and 8-hydroxyl groups, and the *N*-acetamido substituent (Figure 2*b*).

Site-Directed Mutations

The hydrogen bonds and van der Waals contacts between sialic acid and the side chains of HA have also been probed by site-directed mutation of residues in the receptor-binding site (13; Figure 2*a*). Only three mutations abolished erythrocyte binding: Y98F, H183F, and L194A. These results confirm the importance of the Tyr-98 hydrogen bond to the 8-hydroxyl group of sialic acid and the nonpolar contact of Leu-194 to the *N*-acetyl methyl group. His-183 forms hydrogen bonds with both Tyr-98 and to the 9-hydroxyl group of sialic acid. Because changes in Glu-190 and Ser-228, which form hydrogen bonds to the 9-hydroxyl group, had no effect on binding and because other data also indicate that the 9-hydroxyl group is not required for binding (12), it appears that the His-183–Tyr-98 hydrogen bond may be the important interaction. Trp-153 and Tyr-195, which form part of a hydrogen-bonded network with His-183 and Tyr-98, could, however, both be substituted for by phenylalanine with only partial inhibition of binding (13; D Steinhauer, unpublished data)

A Second Sialoside-Binding Site

A second sialoside-binding site is located between subunits of the HA trimer in an interface where two HA1 domains and an HA2 domain make close contact and are known to dissociate when the molecule changes conformation to effect membrane fusion (14). A study of ligand binding to the second site suggested that a substituent that is larger than methyl is required at position 2 but that α(2,6)-sialyllactose does not fit. The affinity of α(2,3)-sialyllactose for the second site was estimated, by collecting X-ray diffraction data at various ligand concentrations, to be at least fourfold weaker than its affinity for the primary site. Because of the way ligands from the second site can extend up toward the first site, it may be possible to construct a bridging ligand as an inhibitor of virus-cell binding that could take advantage of both sites. There is, however, no evidence that the second site is physiologically important, and the fact that α(2,6)-sialosides do not bind argues against its biological relevance.

←

Figure 2 Hemagglutinin receptor binding. (*a*) Schematic diagram of the receptor-binding site of an HA-receptor analog complex, showing the positions of the residues that are changed in site-specific mutants (13) and hydrogen bonds that, in wild-type HA, form with bound sialic acid (*dashed lines*). RBC, Red blood cell; HA, hemagglutinin; WT, wild type. (*b*) Effect of modifications of sialosides on binding to HA. Binding is expressed as affinity (mM). Values determined by NMR (7, 9, 12, 37).

Receptor-Binding Specificity

Two major linkages between sialic acid and the penultimate galactose residues of carbohydrate side chains are found in nature, Neu5Ac α(2,3)-Gal and Neu5Ac α(2,6)-Gal. Different HAs have different recognition specificities for these linkages and the A/Hong Kong/68, X-31 HA binds preferentially to sialic acid in the α(2,6) linkage. By contrast, the HA of a mutant selected by growing X-31 virus in the presence of α-2 macroglobulin, an α(2,6)-linked sialic acid-rich glycoprotein in horse sera (15), has greater affinity than the wild-type HA for α(2,3)-linked sialic acid. The single-amino-acid sequence difference, L226Q, between wild-type and mutant HAs defined the location of the receptor-binding site (16). Comparative X-ray analyses of X-31 HA and mutant L226Q HA in complexes with α(2,6)- and α(2,3)-linked sialyllactose, respectively (4), indicate that residue 226 does not directly contact the sialosides but that the conformation of the receptor-binding pocket is altered by the mutation. Tyrosine 98 and other conserved residues that contact the sialic acid shift ($<$1 Å) as the binding site closes slightly to accommodate the loss of one of the leucine 226 methyl groups. The affinity differences apparently result from these differences in structure.

In a study of sialyloligosaccharide-HA complex crystals, large differences were observed between the bound conformations of α(2,3)- and α(2,6)-linked sialosides (8; Figure 3). A pentasaccharide (LSTc) with an α(2,6)-linked sialic acid binds in a folded conformation, such that the third saccharide, GlcNAc, lies over the sialic acid and makes contact with it (Figure 3). LSTa, an α(2,3)-pentasialoside of the same composition, binds in an extended conformation (Figure 3). The folded conformation appears to be a property of bound α(2,6)-sialosides that contain a NeuAc group on the third saccharide, because an unrelated GlcNAc-containing sialoside inhibitor, 3,6-disialylactoseamine, shows the same folded conformation, whereas the trisaccharide α(2,6)-sialyllactose, identical to the first three saccharides of LSTc but lacking the NeuAc group on the third Glc residue, binds in an extended conformation. The folded sialoside conformation appears to be stabilized by an intramolecular hydrogen bond from the third saccharide, GlcNAc, 3-hydroxyl group, to the ring oxygens of NeuAc, the intervening galactose residue, or the NeuAc glycosidic oxygen and to make intrasaccharide van der Walls contacts from saccharides 1 to 3. The different conformations of the bound α(2,3)- and α(2,6)-sialosides exit the HA binding site in opposite directions (Figure 3). This difference is likely to be an important component of receptor linkage specificity.

Biological Significance of Receptor-Binding Specificity

Two related aspects of linkage recognition specificity have been extensively researched for their biological significance. The first relates to differences observed in the recognition specificities of HAs from viruses infecting different species;

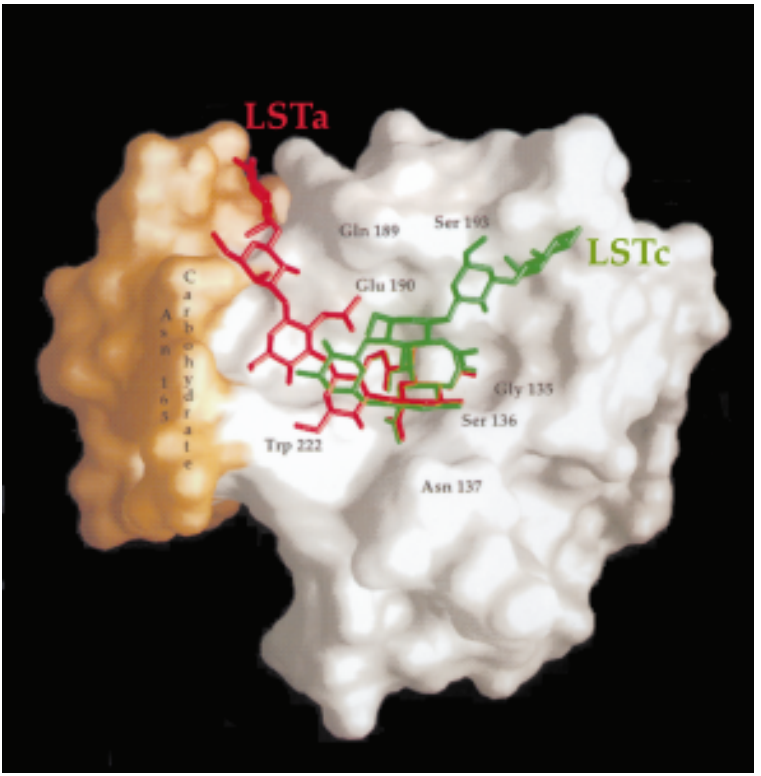

Figure 3 Overlaid images of α(2,6)- and α(2,3)-linked sialylpentasaccharides LSTc and LSTa, respectively, in the HA receptor binding site (8).

viruses from humans recognize the α(2,6) linkage, those from avians and equines recognize α(2,3) linkages, and those from swine appear to recognize both (17–21). These differences may be important in limiting the transfer of viruses between species and were analyzed especially in relation to the emergence of new pandemic viruses in humans. In the first years of the Asian and Hong Kong pandemics, both of which were probably caused by the introduction of viruses containing avian HAs into the human population, viruses with either α(2,6)- or α(2,3)-recognition specificity were identified, suggesting a gradual change in specificity (17, 20). The failure, in 1997, of the outbreak of H5 avian influenza to spread within the Hong Kong population may also have been related to the inappropriate α(2,3)-receptor binding specificity of the virus involved (22).

In humans, horses, and pigs, influenza is a respiratory infection; in avians, it is enteric. Experiments with linkage-specific lectins have shown an abundance of sialic acid in α(2,6) linkage in human lungs (23) and of sialic acid in α(2,3) linkage

in bird intestine; in pigs, both linkages were detected in respiratory tract cells (21). In addition, mucins from human lung are reported to be rich in α(2,3)-linked sialic acid, which would inhibit cell receptor recognition by α(2,3) linkage-specific HAs (24), and, by contrast, equine fluids may be rich in nonspecific inhibitors containing sialic acid in α(2,6) linkage (15, 25). The nature of the sialic acid linkage on cells, the action of these soluble inhibitors, or both appear to be involved in selecting HAs with different linkage recognition specificity.

The molecular basis of the differences in receptor-binding specificity between H3 subtype viruses isolated from humans and avians has been addressed by sequence analysis as in the laboratory-selected mutant L226Q (16). Residue HA1 226 again appears to be involved, and HA1 228 has also been linked with specificity differences. The HAs of viruses from humans that preferentially recognize the α(2,6) linkage contain leucine and serine at 226 and 228; the HAs of avians contain glutamine and glycine at the equivalent positions (5, 18, 26, 27). Hemagglutinins of the H1 subtype differ in this respect; human and avian isolates also recognize α(2,6) and α(2,3) linkages, respectively, but both of their HAs contain glutamine at HA1 226 and glycine at HA1 228. Other residues in HAs of this subtype, including 186 (Pro in avian; Ser in human) and 225 (Gly in avian; Asp in human) (20), influence receptor specificity. Within the H3 subtype, residues in addition to 226 and 228 have been shown to affect linkage recognition specificity (22, 28); differences at residues HA1 218 and 193, for example, in the vicinity of the receptor-binding site, have been linked with differences in specificity (29). The structural consequences of these amino acid substitutions have not been determined.

A second aspect of research on the biological significance of receptor binding specificity concerns similar selection processes during virus replication in different cells in vitro and is relevant for both influenza surveillance and vaccination. Internationally, viruses are collected from outbreaks of influenza to screen for changes in the antigenic properties of HAs that might influence the effectiveness of vaccination. To obtain material for analysis the viruses are grown in either mammalian cells or embryonated hens' eggs, and it has been appreciated for many years that these different systems can result in the propagation of related but distinguishable viruses. It is important, particularly because hens' eggs are universally used in vaccine production, that antigenic differences can on occasion be detected when the same viruses are grown in different cells (e.g. 30), and the question arises, how closely representative are the isolated viruses of the viruses in circulation (e.g. 31)? Sialic acid linkage differences may be involved in this selection process because mammalian cell surfaces contain sialic acid in α(2,6) linkage and the chorioallantoic membranes of hens' eggs are rich in sialic acid in α(2,3) linkage (32, 33). The process of selection is, however, not simply based on these differences because, although a clear preference of avian viruses for hens' eggs has been observed (34), the HAs of viruses from humans, which have α(2,6) linkage recognition specificity, function effectively in hen egg infections. The covariation of differences in antigenicity and receptor-binding specificity is presumably related to the location

of the conserved receptor-binding site, closely surrounded by antigenically important variable residues that occasionally influence receptor-binding affinity or specificity (35).

Receptor Affinity and Inhibition of Receptor Binding

Differences in receptor-binding specificity are most clearly shown in hemagglutination assays with specifically derivatized erythrocytes (36) or by inhibition of hemagglutination by multiple-sialylated molecules such as α2-macroglobulin (15, 25). In such competitive assays for example, X-31 had about eightfold greater affinity for the α(2,6)-linked sialylpentasaccharide LSTc than the α(2,3)-linked pentasaccharide LSTa (37). Direct NMR estimates of differences in affinity of isolated HAs indicate appropriately specific but small differences between HAs of X-31 virus, which, in hemagglutination assays, prefer α(2,6) linkage, and HAs of the mutant L226Q, which bind instead to α(2,3)-sialoside–derivatized erythrocytes. Thus, for X-31 the dissociation constants for sialylactoses were determined to be 2.1 mM for α(2,6)- and 3.2 mM for α(2,3)-sialolactose, respectively; for the L226Q mutant HA, dissociation constants were 5.9 mM and 2.9 mM (9), respectively. These measurements also indicate that the affinity of HA for sialosides is low, implying that tight binding of viruses to cells during infection is mediated by the simultaneous interaction of a number of HA molecules. Large increases in binding affinity of HA rosettes with multiple binding sites for polyvalent sialosides have, in fact, been measured by surface plasmon resonance (38), and similarly large differences between viruses binding to monovalent and polyvalent sialosides have been recorded (19).

The influence of cooperativity on effective binding affinity and specificity that these results imply has encouraged studies of the inhibition of receptor binding by modified sialosides that could be used as polyvalent inhibitors (39–42).

X-ray structures have also been determined for four high-affinity ligands in complexes with HA, including one to 2.1-Å resolution with a compound that has a 50-fold greater affinity for HA than 2-*O*-methylsialic acid (6). Two of the ligands have large napthyl rings attached by 10- and 8-atom linkers to the glycosidic (2-) position of sialic acid. These bind with 50- and 25-fold-higher affinity (40 μM and 80 μM, respectively) than 2-*O*-methylsialic acid (2 mM). The structures show the sialic acid bound as in other sialosides with the methylene linker and napthyl ring extending down a primarily apolar channel adjacent to the receptor-binding site. The amido portion of the longer, 10-atom linker appears to form a hydrogen bond to the carbonyl of Arg-224 of HA, which may account for part of the difference in the affinities. The increased binding affinity of these two ligands appears to be caused by the napthyl interaction with HA, because similar linkers terminating in a methyl group show no increase in affinity compared with 2-*O*-methylsialic acid and a nonspecific hydrophobic effect (desolvation) seems unlikely because phenyl and napthyl rings on shorter linkers or at other positions (4-phenylpropionyl) show only small increases in affinity (14).

ANTIGENIC VARIATION

Anti-HA antibodies neutralize virus infectivity. As a consequence, changes in HA structure that prevent antibody binding are required for the generation of viruses with the potential to cause new epidemics. During such antigenic drift, the HAs of viruses of the Hong Kong pandemic isolated between 1968 and 1999 have accumulated amino acid substitutions at a rate of ∼3.5 residues per year (43). More than half of the changes detected (60 of 101) are retained in HAs of viruses isolated in subsequent years; most of these (57 of 60 between residues HA1 50 and 280) involve residues on the membrane-distal surface of HA, whereas about two thirds of those not retained (27 of 41) are buried (K Cameron, YP Lin, AJ Hay, unpublished data). These data suggest that retained substitutions may have been selected because they prevent antibody recognition. This inference is supported by the coincidence of their locations, with substitutions detected in antigenic variant HAs selected by growing H3 subtype viruses in the presence of anti-HA monoclonal antibodies (2).

Antibody-Binding Sites

The sites of these monoclonal antibody-selected substitutions indicate the sites at which the selecting antibodies bind (2, 44). This definition of antibody-binding sites is supported by X-ray crystallographic studies of the five antibody-selected mutant HAs, G146D (45), G135R, (7), Q189K (W Weis, JJ Skehel, DC Wiley, unpublished data), S157L (46), and T131I (47), all of which exhibited only local changes in the HA structure and therefore defined the location of the monoclonal antibody-binding site. This definition was also supported by electron micrographs of HA in complexes with monoclonal antibodies of defined recognition specificity (48) and by direct X-ray studies of three crystalline complexes of two monoclonal antibody Fabs with HA (46, 47, 49; Figure 4).

Antigenicity

Examination of the sites of amino acid substitution in natural and monoclonal antibody-selected antigenic variants indicates that all are on the surface of the membrane distal HA1 domain predominantly surrounding the receptor-binding site. Two features of the antigenic sites are particularly notable: the looplike structure of several of them and the incidence of carbohydrate side chains. Protruding loops close to the receptor-binding site of A/Hong Kong/68 HA, residues 140–146 and 155–164, were suggested to be particularly important as antibody-binding sites (44) and appeared to be suited for avid antibody binding because they projected from the HA surface. They could accept amino acid substitutions without affecting the framework of the HA, and all of the residues in the loops, from 142 to 146 and 155 to 160, have changed in the HAs of viruses isolated between 1968 and 1999, some on multiple occasions. Prominent structural loops have also been found to form antibody-binding sites in, for example, influenza neuraminidase

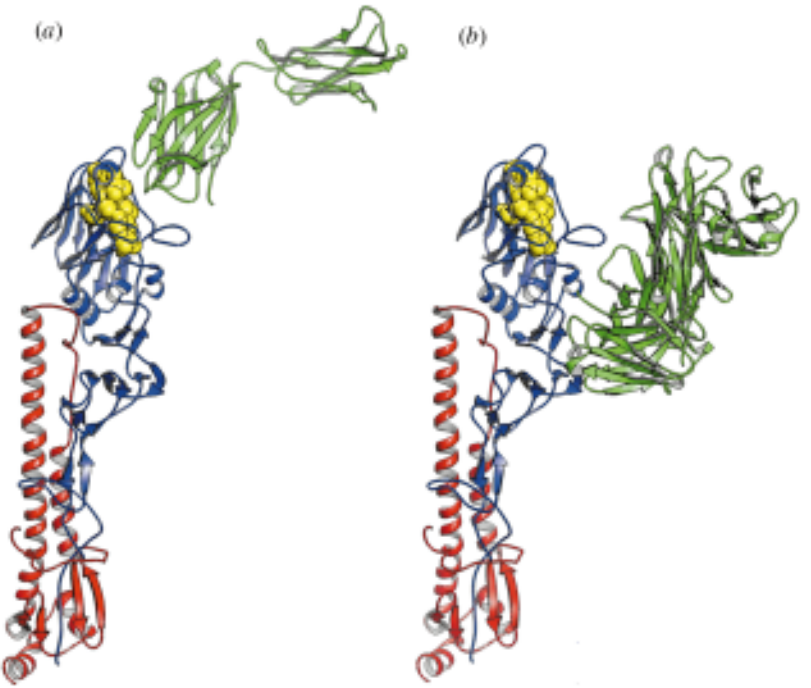

Figure 4 Complexes between Fab fragments of two neutralizing monoclonal antibodies, HC19 and HC45, with X-31 HA. (*a*) HC-19 Fab covering the receptor-binding site. (*b*) HC-45 Fab bound below the receptor-binding site. Receptor-binding-site residues are shown as *spheres*. (Adapted from 49).

(NA) (50) and picornaviruses (51, 52) and have been proposed for HIV-1 gp120 (53).

Oligosaccharide attachment provides two mechanisms for evading immune responses, both of which are observed with the HA: First, portions of the HA surface are covered by carbohydrate side chains that are synthesized by cellular enzymes and are, therefore, antigenically "self" and do not induce antibodies; second, during antigenic drift, amino acid substitutions create new oligosaccharide attachment sites in antibody-binding regions, generating resistance to antibody binding. The first mechanism was illustrated by the finding that a large surface of the A/Hong Kong/68 HA, covered by the oligosaccharide attached at N165, was invariant during antigenic drift between 1968 and 1979 (see Figure 6b of reference 2). The second mechanism was suggested by observations that substitutions with the potential to generate oligosaccharide sites were located in antibody-binding regions of both H3 and H1 subtype HAs (44, 54–56) and was demonstrated experimentally in two ways: (*a*) When a single-residue-variant HA (D63N) containing a new oligosaccharide attachment site at HA1 Asn-63 was synthesized in the presence

of tunicamycin to block glycosylation, it was shown to revert to binding the monoclonal antibody that had been used to select it (57); (*b*) the HAs of the epidemic viruses of 1969 and 1975, which, unlike A/Hong Kong/68, are glycosylated at HA1 63, also failed to bind this monoclonal antibody but were shown to bind it after synthesis in tunicamycin (57). This indicates that preventing glycosylation of the 1969 and 1975 HAs reexposed an epitope of the 1968 HA that had been buried during antigenic drift by the introduction of the glycosylation site at HA1 63.

Since the beginning of the H3 epidemics in 1968 and continuing to date, there has been a large increase in the number of oligosaccharide attachment sites on HA1. The HA of the 1968 Hong Kong influenza virus contained six oligosaccharide attachment sites at HA1 residues 8, 22, 38, 81, 165, and 285, the last three of which are on the membrane-distal surface of HA (58). By 1999, HA1 contained 10 oligosaccharide attachment sites (residues 8, 22, 38, 63, 122, 126, 133, 165, 246, and 285), 7 of which have accumulated in the antigenically important membrane-distal region (K Cameron, YP Lin, AJ Hay, unpublished data). Retroviral and filoviral envelope glycoproteins are even more highly glycosylated than HA (e.g. see 59), and antigenically distinct HIV-1 and SIV-1 strains differing in glycosylation have been described (60, 61).

Antibody Binding and Neutralization of Infectivity

The relationship between antibody binding, neutralization, and the mechanism of escape from neutralization by mutation has been addressed by structural studies of HA complexes with two Fabs from neutralizing monoclonal antibodies (46, 47, 49). One Fab, which binds over the receptor-binding site, directly contacts three of the conserved residues that bind the receptor sialic acid and neutralizes virus infectivity by directly blocking virus-cell binding (Figure 4*a*). Escape mutants have been shown either to interfere sterically with Fab binding [e.g. S157L (46)] or to cause local conformational changes (T131I) that must be distorted back to a wild-type-like conformation to bind the Fab at a cost in free energy resulting in reduction in binding affinity by 4000-fold (47). A second Fab binds 17 Å below the HA receptor-binding site (Figure 4*b*) but also neutralizes infectivity by blocking receptor binding, although indirectly through the bulk of either the Fab or immunoglobulin molecule. No conformational changes are observed linking antibody binding to the distant receptor-binding site, so that antibody-mediated neutralization and inhibition of hemagglutination appear to result from antibody blocking (49).

The efficiency of neutralization by both of these monoclonal antibodies was shown to depend directly on their avidities for virus; the antibody that binds at the membrane-distal tip of HA binds more avidly and neutralizes more efficiently even though its affinity for HA is less than one tenth that of the antibody that binds below the receptor-binding site (49). Escape mutations in the antigenic drift since 1968, are found both near to and distant from the receptor-binding site. The studies of the avidity and neutralization by these two monoclonal antibodies suggest that the antibodies that bind to all of these sites will neutralize by blocking receptor binding

and will vary in effectiveness by their avidities for virus, regardless of the locations of the sites. Further discussion of the relationship between antibody-binding sites and escape mutations for influenza and other viruses (46, 47, 49, 62, 63) has included considerations of the size differences between antibody footprints and the receptor-binding site. In addition, observations have been made that, because only a few of the many residues in a protein-protein interface contribute most of the free energy (e.g. 64), antibody- and receptor-binding sites can geometrically overlap completely but still be susceptible to escape mutations if the subset of residues that are energetically important for antibody binding are not identical to those necessary for receptor binding (62).

Antigenic Subtypes

Influenza type A viruses are subtyped by the antigenic properties of both of their membrane glycoproteins, HA and NA. In viruses that infect avian species, 15 subtypes of HA and 9 of NA have been identified. Of the 15 HA subtypes (H1–H15), H3 and H7 also infect equines; H1, H2, and H3 infect humans; and at least four, H1, H2, H3, and H9, infect swine. In addition, small numbers of isolates of avian viruses are occasionally made from humans such as, for example, from the outbreak of H5 influenza in Hong Kong in 1997 (65, 66) and the isolates of H9 influenza in 1998 (67, 68). Within a subtype, as described above for the H3 subtype of human influenza, the amino acid sequence of HA has been observed to vary up to 20%; between subtypes sequence identity ranges from 70%–30% (5, 69, 70). HA1 domains are more variable than HA2, consistent with their antigenic properties.

MEMBRANE FUSION AND VIRAL ENTRY

Hemagglutinin Precursor HA0

HA is synthesized as a precursor, HA0, that trimerizes in association with chaperones in the endoplasmic reticulum and is transferred through the Golgi apparatus to the cell surface (e.g. 71–73). Cleavage of HA0 generates the C terminus of HA1 (residue 328 of HA0) and the N terminus of HA2 and is required for membrane fusion activity and infectivity (reviewed in 2). In HA0s from 13 of the 15 HA subtypes, the HA1 and HA2 polypeptide chains are separated by a single arginine residue, which is eliminated from the C terminus of HA1 by a virion-associated carboxypeptidase after cleavage (74). Cleavage occurs at the cell surface or on released viruses. For the HA0 of the H1, H2, and H3 subtype viruses that have caused epidemics, cleavage may be mediated by the serine protease, tryptase Clara, produced by Clara cells of the bronchiolar epithelium (75). This enzyme shows recognition specificity for the sequence Q/E-X-R found at the cleavage sites of these HAs. The proteases responsible for cleavage of the HA0s of enteric avian viruses are not known. For some of the HAs of the H5 and H7 subtypes, the HA1 and HA2 polypeptide chains are separated by polybasic sequences that are

inserted at the cleavage site (76–78). In these cases, cleavage is intracellular and involves subtilisin-like enzymes that are active in the post-translational processing of hormone and growth factor precursors (79, 80). The furin recognition sequence R-X-R/K-R is a common feature of the inserted polybasic sequences. The wide tissue distribution of furin-like enzymes and the efficiency of intracellular compared with extracellular cleavage appear to be related to the widespread systemic and virulent infections caused by the H5 and H7 viruses in birds and the localized outbreak in Hong Kong, in 1997, of severe respiratory infection by an H5 virus in humans (reviewed in 81).

HA0 Structure

The structure of the uncleaved HA0 of A/Hong Kong/68 virus was determined crystallographically by using a mutant HA, R329Q, to prevent its cleavage into HA1 and HA2. Only 19 residues near the cleavage site are positioned differently in uncleaved HA0 compared with cleaved HA; the remaining structures are essentially superimposable (cf Figure 1*a* and *b*). These residues, HA1 323–328, R329Q, in the mutant HA0 used for analysis and 1–12 of HA2 form a loop that projects the eight residues at the cleavage site, HA1 327 to HA2 5, away from the surface of the molecule (82).

A negatively charged cavity is found adjacent to the loop, into which HA2 residues 1–10, the fusion peptide, inserts after HA0 cleavage, possibly guided by an electrostatic force generated when the positively charged amino terminus of HA2 is formed (Figure 5*a* and *b*). The cavity contains aspartic acids HA2 109 and 112 and histidine HA1 17, which, on cleavage, are buried without pairing to other ionizable residues; the aspartates form 5-hydrogen bonds with the main-chain amide groups of HA2 residues α(2-6) and histidine HA1 17 forms a hydrogen bond through a water molecule to the carbonyl oxygen of HA2 10. Two HA1 C-terminal residues, glutamic acid HA1 325 and arginine HA1 321, move out of the cavity on cleavage.

HA0 Cleavability and Virus Pathogenicity

The structure of HA0 provides explanations for the correlation of precursor cleavability with pathogenesis (80, 83). On one hand, it indicates that the side chain of the P-4 residue is packed against the HA0 structure and would not be accessible for binding into a recognition site as furin activity appears to require. On the other hand, insertion of four residues at the cleavage site would project the site into solution and expose the inserted P-4 residue. Some H5 subtype HAs lack a furin recognition site but are nevertheless associated with high pathogenicity. In some of these cases the HAs lack a carbohydrate side chain (84, 85) normally located 14 Å membrane distal to the cleavage site, which could influence the accessibility of the site to proteases (Figure 1). In other cases, the HAs contain basic amino acid substitutions at P-5 and P-6 (86, 87), which may perturb the structure of HA0 and, as a consequence, increase protease accessibility.

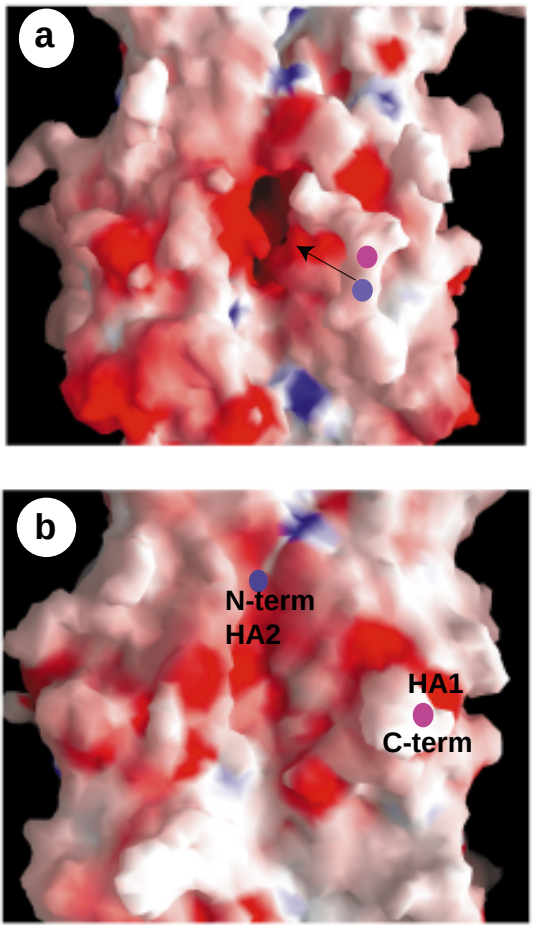

Figure 5 Surface cavity in HA0 adjacent to the cleavage site is filled by the fusion peptide after cleavage. (*a*) Surface of R329Q HA0 trimer with cavity at *arrow*. The cleavage site is on the loop between the dots that label the HA1 C terminus and HA2 N terminus. The cavity surface is ~10 Å wide and 30 Å long. (*b*) Cleaved BHA surface showing separation of the newly created termini. Of solvent-accessible surface area of the R329Q HA0 cavity and of the fusion peptide, 797 $Å^2$ and 1380 $Å^2$, respectively, are buried per monomer, as a result of the cleavage and subsequent rearrangement shown in Figures 1*a* and *b*.

Priming and Activation of Membrane Fusion Potential

As a result of HA0 cleavage, HA is primed for activation of its membrane fusion potential at endosomal pH in the next cycle of infection. It seems possible from the structure of HA0 that the movement of the fusion peptide into the charged cavity

in HA0, burying the ionizable residues, may be the priming event. Amino acid substitutions at each of the charged residue positions have been found in mutant HAs that fuse membranes at higher pH than wild-type HA (88, 89).

At the beginning of the next infection, receptor-bound virus is taken into cells by endocytosis and at the low pH of endosomes, between pH5 and pH6, HA-mediated fusion of the viral and endosomal membranes is activated (90–92). A fusion pH-induced, irreversible conformational change in the HA exposes the HA2 N-terminal fusion peptide, while preserving the structure of the HA1 receptor-binding domain (9, 46, 93). Experiments with photoreactive phospholipid-labeling reagents (94–96) and studies of HA aggregation, liposome association, and protease susceptibility at fusion pH (93, 97) support a model in which the exposed fusion peptide inserts into the cellular membrane, anchoring HA into both pre-fusion membranes; by its N terminal in the endosomal membrane and by its C terminal in the virus membrane (93, 98, 99).

Activation pH and Temperature

Membrane fusion activity and changes in HA conformation co-vary with pH and temperature (100). X-31 HA, for example, fuses membranes at pH 5.6 at 37°C and at pH 7.3 at 62°C. HA mutants that are selected by growing influenza viruses in the presence of amantadine, to increase the pH of endosomes, fuse with membranes at higher pH than wild-type virus (88), and mutants with similar properties are also obtained by passage of influenza viruses in MDCK cells (89, 99, 101). An approximately linear relationship is observed between temperature of fusion at pH 7.3 and pH of fusion at 37°C for mutants that fuse between pH 6.4 and pH 5.6 at 37°C (102). These studies indicated that both low pH and high temperature can trigger fusion activity. They also revealed that large changes in the thermal stability of HA were induced at fusion pH, which led to the conclusion that in the neutral-pH-conformation HAs are relatively unstable and that the instability is specifically relieved at the pH of fusion (102). These observations and conclusions have been confirmed (103), although differences in HA structure that occur at fusion temperature at neutral pH by comparison with those that occur at fusion pH at 37°C (102) were not detected when different proteolysis assays were used to analyze the heated molecules (103).

Refolding of Viral Hemagglutinin at Fusion pH

The X-ray crystal structure of TBHA2, a proteolytic product of low-pH-treated viral HA (104), defined the details of the low pH-induced conformational rearrangement throughout the length of HA2 (Figures 1*c* and 6). Three major refolding events occurred (Figure 7). (*a*) An extended loop and short α helix became an extension of the central triple-stranded coiled coil found in native HA (residues 76–105 extended to residues 38–105), relocating the fusion peptide over 100 Å from its previously buried position. This coiled-coil structure had been predicted

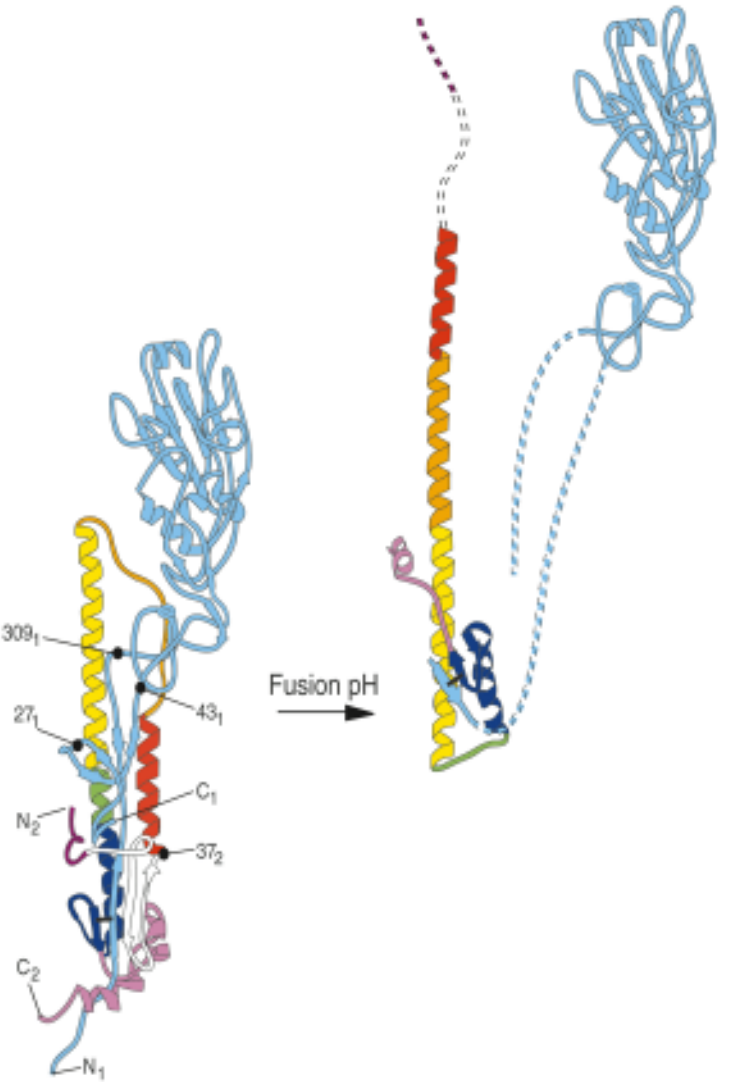

Figure 6 The ectodomain of HA in the neutral-pH- and fusion pH-induced conformations, indicating the N and C termini of HA1 and HA2, N1, C1, N2, and C2. The sites of proteolytic digestion exposed at fusion pH, HA1 residue 27 and HA2 residue 37, are recognized by LysC and thermolysin, respectively, and HA1 residues 43 and 309, beyond which HA1 is disordered in the Fab-HA1 28-328 crystal structure. HA2 is shaded to explain the fusion pH-induced changes in structure. The discontinuous lines indicate parts of the structures that are unknown (46, 104).

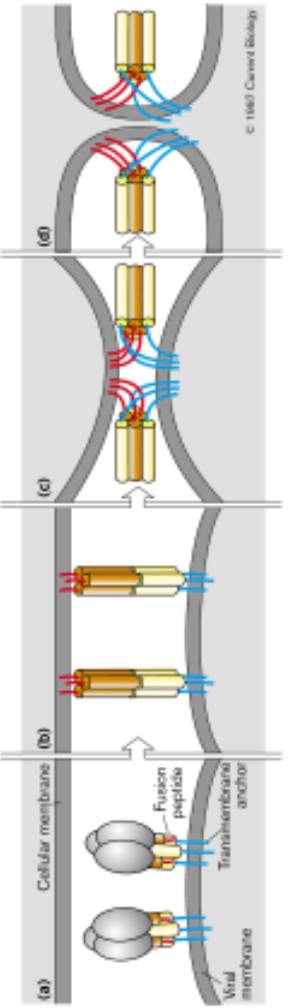

Figure 7 Hypothetical mechanism for membrane fusion by virus glycoproteins. (*a*) The entire HA molecule. (*b–d*) The HA2 subunits alone, in which the termini of the proteins come into relative proximity, thereby inducing membrane fusion. (Adapted from 108a).

from sequence analyses (105, 106) and was proposed to be formed at low pH from studies of synthetic peptides (107). (*b*) The middle of the long α helix of native HA2 unfolded to form a reverse turn, and the second half of the long α helix jackknifed back to lie antiparallel against the first half, also relocating C-terminal residues by >100 Å in relation to coiled-coil residues 76–105, which form a common structure in both conformations. (*c*) Residues 141–175, located C terminal to a small β-sheet hairpin that accompanied the jackknifed α helix, appeared to be extruded from their compact association in HA2 to become a mostly extended structure that reached back up the central coiled-coil, packing antiparallel within the groove between adjacent α helices. The overall effect of this refolding is apparently to deliver the fusion peptide toward the target membrane and to bend the molecule in half so that the fusion peptide and the viral membrane anchor are near the same end of the rod-shaped molecule (108; Figures 6, 7). Subsequently, a number of other viral glycoprotein fragments and the SNARE complex involved in synaptic vesicle fusion have all been shown to share a coiled-coil architecture, with both membrane-interacting segments at one end (Figure 8; reviewed in 109).

Recombinant HA2 Spontaneously Adopts the Fusion pH Conformation

The stability of the trimeric coiled-coil-based TBHA2 structure suggested that it might fold spontaneously if HA2 were expressed in bacteria, in the absence of HA1, the nonpolar fusion peptide and the C-terminal membrane anchor (EBHA2) (110; Figure 9). Purified EBHA2 was trimeric by chemical cross-linking and gel filtration, highly helical by circular-dichroism measurement, melted at a high temperature like TBHA2 (102), bound low-pH conformation-dependent HA antibodies like TBHA2 (111), yielded specific proteolytic dissection products previously characterized from viral TBHA2 (111), and appeared as rods in electron micrographs, indistinguishable from those of TBHA2 (97), all indications that EBHA2 had folded spontaneously in bacteria into the same soluble trimeric structure as low-pH-treated viral HA (110). An X-ray structure of a related molecule (see below) establishes that the structure of EBHA2 is like TBHA2 (112).

The observation that EBHA2 folded spontaneously at neutral pH into the fusion-pH-induced conformation added to the evidence that the fusion-pH conformation is the lowest free-energy state of HA2. This is consistent with a model of cleaved HA as a metastable intermediate in which extensive contacts between HA1 and HA2 kinetically trap the molecule behind a free-energy barrier that low pH lowers or surmounts to yield the stable fusion pH conformation (104, 110).

HA2 expression in bacteria (110), by showing that a fusion conformation will form spontaneously in the absence of the glycoprotein's receptor-binding domain, provided the rationale for expression of recombinant membrane fusion subunits of other viral glycoproteins to study their membrane fusion conformation. Because structures that are analogous to the neutral-pH HA conformation are not available for other fusion glycoproteins, it is only for HA that experiments have demonstrated that the conformational change triggered either in vivo or in vitro

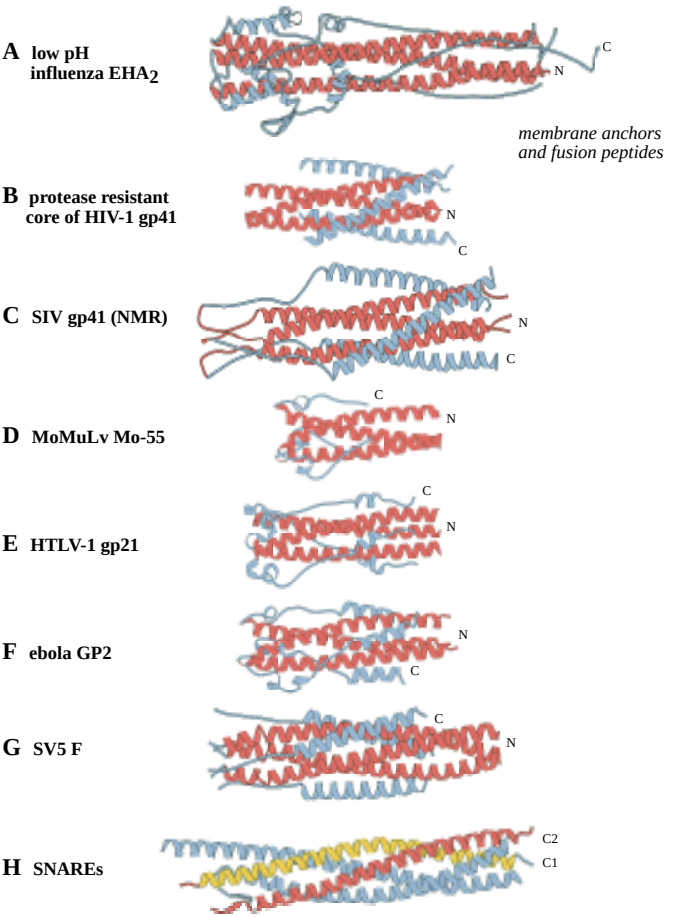

Figure 8 Rod-shaped α-helical bundles of the ectodomains of membrane fusion proteins, with the regions that insert in the participating membranes at one end (righthand). (*A*) Fusion pH influenza virus HA after proteolytic cleavage at HA1 residue 27 and HA2 residue 37, which removes the bulk of HA1 (residues 28–328) and the fusion peptide region HA2 (residues 1–37) (104). (*B*) Recombinant, proteolysis-resistant core of HIV-1 gp41 (see 108 and references therein). (*C*) Recombinant SIV gp41 (115). (*D*) 55-residue recombinant fragment of Moloney murine leukemia virus TM subunit (117). (*E*) Recombinant gp21 of HTLV-1 (118). (*F*) Recombinant Ebola virus GP2 (121). (*G*) Recombinant SV5 F1 (114). (*H*) Recombinant synaptic fusion complex with the *v*-SNARE synaptobrevin ectodomain, *t*-SNARE syntaxin C-terminal ectodomain, and the two helical regions of the *t*-SNARE SNAP-25B (124). *C1* and *C2* label the C termini that are inserted, prefusion, in the plasma and vesicle membrane, respectively. This figure, modified from reference 121, was generated with RIBBONS (203).

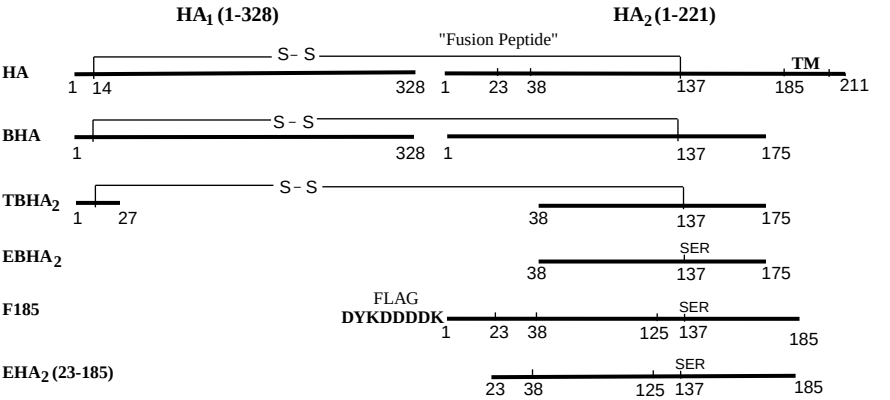

Figure 9 Schematic of HA and HA2 sequences. EHA2 (*Escherichia coli*-expressed HA2 residues 23–185) is the structure determined crystallographically and shown in Figures 8 and 9. TM, Transmembrane anchor; S–S, interchain disulfide bond from HA1 Cys-14 to HA2 Cys-137; $CYKDDDDK_1$, FLAG octapeptide (in F185).

reaches the same conformation (TBHA2) as recombinant expression (EBHA2) achieves spontaneously.

A test of the restoration of bacterially expressed HA membrane interactions was made by reintroducing the N-terminal fusion peptide, solubilized by an upstream highly charged octapeptide FLAG (DYKDDDDK) (113; Figure 9). The full ectodomain 1–185 of HA2, with FLAG upstream (called F185) also folded spontaneously into soluble trimers in the low-pH–induced conformation, as characterized by the same methods as those used on EBHA2 and discussed above. Removing the FLAG peptide with enterokinase generated the same hydrophobic properties that were found earlier with low-pH-treated HA: The molecule with its FLAG removed aggregated into rosettes or bound to detergent micelles or lipid vesicles. Furthermore, subsequent removal of the fusion peptide by thermolysin reversed these hydrophobic properties, as observed earlier in the generation of TBHA2 from viral HA. These observations indicated that the bacterially expressed conformation with an intact fusion peptide could mimic the membrane interaction properties of low-pH-treated viral HA.

COMPARISONS WITH OTHER VIRUS AND CELLULAR MEMBRANE FUSION PROTEINS

An important development in the membrane fusion field recently is the remarkable similarity to the fusion pH-induced conformation of TBHA2 that has been found in recombinant ectodomains or peptide fragments of the fusion proteins of other viruses (reviewed in 109) from diverse families, including the retroviruses

Moloney murine leukemia virus, human immunodeficiency virus (HIV)-1, simian immunodeficiency virus (SIV)-1, and human T-cell leukemia virus (HTLV)-1, the filovirus, Ebola virus, and the paramyxovirus SV5 (108, 114–121; Figure 11). Equally remarkable, a related rod-shaped structure has been found for the *v*- and *t*-SNARE complex involved in synaptic fusion (Figure 8; reviewed in 109, 122–124). In each case the termini expected to be embedded in the two prefusion membranes are found at one end of a rod-shaped molecule containing an α-helical coiled coil. The formation of these rodlike structures has been suggested to provide both a mechanism for the close apposition of the prefusion membranes and a driving force for the fusion of the bilayers (108, 124, 125).

Although all of the viral membrane fusion ectodomain structures share a triple stranded α-helical coiled coil to which the N-terminal fusion peptide would be attached, they differ in the structure of the loop at the opposite end of the rod and in the structure of the antiparallel outer layer that binds along the outside of the core coiled coil. The transmembrane (TM) proteins of Moloney leukemia virus and HTLV-1 and the filoviral GP2 glycoprotein structures (Figure 8) are extremely similar to each other (117–119, 121), sharing details in the coiled-coil packing such as an axial chloride binding site, having a homologous loop structure as predicted from the 40%–50% sequence identity of a 25-residue segment (59), and having an outer layer with a stretch of extended chain followed by a short α-helical segment (118, 119, 121). The gp41 ectodomains of HIV-1 and SIV also have an outer layer with a short extended segment but with a longer α helix (e.g. $>$45 residues in SIV gp41 vs 28 residues in GP2) (108, 121) and apparently a different loop structure (see discussion in 118), observed so far only by NMR of a mutant molecule with the paired cysteines replaced by serines (115).

An additional functional role for the loop at the opposite end of the trimeric rods from the membrane-interacting segments for all of these molecules is suggested by analogy to HA, in which this is the site at which the receptor-binding domain HA1 is disulfide bonded to HA2. In the fusion pH conformation, the receptor-binding domain is directed away from the membrane-proximal, fusion site end of the rod. The structure of Ebola GP2 (121) suggests that the GP1 receptor domain may also be disulfide bonded to that end of the rod and be similarly directed away from the membrane interaction site, permitting the close apposition required for membrane fusion. Similar arrangement may exist for some retroviruses like Rous sarcoma virus (RSV) and the avian leukosis and sarcoma virus (ALSV) based on sequence homology (121). Biochemical and antigenic data indicate that this loop-end of the gp41 rod interacts noncovalently with the receptor-binding subunit gp120 (126–128), so that this arrangement may apply to the lentiviral glycoproteins as well.

The ectodomain structure of the F1 subunit of the paramyxovirus SV5 is similar to the other virus fusion proteins (Figure 8), but the loop between the inner and outer layers of the rod contains a 250-residue segment that is missing from the determined structure (114). Whether this segment is involved in sensing a trigger for a conformational change to cause membrane fusion is unknown. In F1, α helices extend all the way into the fusion peptide and to within five residues of the

C-terminal membrane anchor. Furthermore, up to six residues can be deleted between the C-terminal anchor and the ectodomain without inhibiting fusion activity (114). These observations suggest that, in this case, no flexible linkers are found between the α helices and the N- and C-termini, which has implications for fusion mechanisms (114).

THE MECHANISM OF MEMBRANE FUSION

Fusion Peptide Insertion

The HA2 N-terminal fusion peptide is the most highly conserved region in HA. It is, however, clear from mutant analyses that a number of residues in this region can be substituted without loss of fusion activity and that others cannot (71, 88, 129–131). Substitution of the N-terminal glycine by residues other than alanine led to inefficient in vitro fusion (130, 131), although N-terminal leucine has been found in thermolysin-dependent mutant viruses (132). Deletion of the N-terminal glycine prevents fusion as also does deletion of leucine at position 2 (130, 133), suggesting that fusion peptide length is critical for fusion activity, and the observations that fusion peptide length is maintained by leucine insertion in the thermolysin-dependent mutants (132) supports this suggestion. A mutant in which the N-terminal glycine is replaced by serine apparently causes hemifusion (131). Glycine residues are found at ~4-residue spacing in fusion peptides of HA and other virus fusion proteins (e.g. 134); only the glycine at residue 8 was found to be essential for the fusion activity of HA (130). Two charged residues, HA2 E11 and E15, were found not to be essential and could be substituted simultaneously by valine with no effect on fusion (130). At neutral pH, the fusion peptide is buried in a pocket of ionizable residues adjacent to the site of precursor cleavage. Incubation at fusion pH releases the peptide from this buried position and causes its insertion into the target membrane, which has been demonstrated directly by using hydrophobic photolabels (94–96). Only residues 1–22 of HA2, including the fusion peptide, were labeled, indicating that no other region of HA in the fusion pH conformation was inserted into the membrane (96).

Intermediates in Membrane Fusion

An unusual N-cap domain, terminating the central N-terminal coiled coil of the fusion pH conformation of HA and tying the N- and C-terminal membrane-proximal segments of the molecule together, was observed in the crystal structure of a construct of HA2 called EHA2(23–185) (112; Figures 9 and 10). Unlike the other amide groups in α helices, three amides at the N terminal of an α helix do not form hydrogen bonds with carbonyl residues of preceding residues in the helix. As a consequence, α helices are often stabilized and terminated by adjacent residues, sometimes negatively charged, which are termed the N cap, that form hydrogen bonds with these unpaired amide groups (135, 136). The four residues 34–37 of

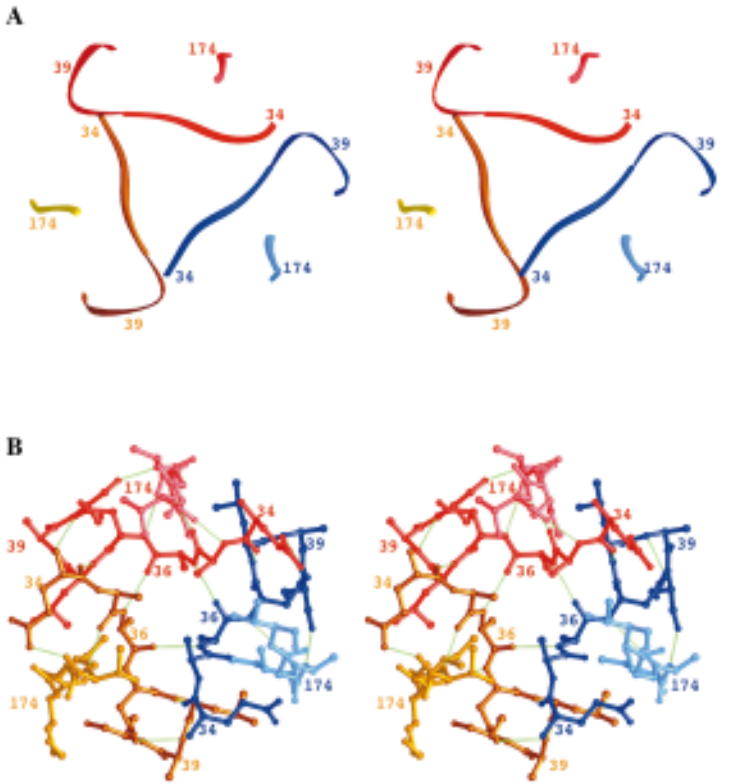

Figure 10 N-cap domain of EHA2(23–185). (*A*) Stereo ribbon diagram of the N-terminal and the C-terminal residues of EHA2(23–185), viewed down the molecular threefold symmetry axis. (*B*) Stereo atomic diagram of the N-terminal residues (view as in *A*) and the C-terminal residues of EHA2(23–185). *Dashed lines* are potential hydrogen bonds.

HA2 appear to have evolved both to cap the N terminus of the core α helix and to terminate the triple-stranded coiled coil. Proceeding N terminally, the last helical residue is leucine 38. The aspartic acid side chain of residue 37 forms a hydrogen bond to the two terminal amide groups at residues 39 and 40, serving as an N cap. Segment 34–37 then crosses (clockwise, Figure 10*A* and *B*) to cap the neighboring α helix of the three-stranded coiled coil by forming a hydrogen bond from the carbonyl group of residue 34 to the third free helical amide group, that of residue 38 (Figure 10*B*).

The three N-capping segments (residues 34–37), as they extend laterally to the adjacent helix, also interact with each other around the threefold molecular symmetry axis to form a small annulus (Figure 10*A* and *B*). The annulus is stabilized by the threefold contacts among the methyl groups of alanine 36 from each monomer, forming a nonpolar layer around the trimer axis and another similar layer from

alanine 35 stacked on top of it. Three symmetric hydrogen bonds cycle around the trimer axis from the carbonyl group of residue 36 in one monomer to the amide group of the same residue (residue 36) on the next monomer counterclockwise around the threefold axis (Figure 10*B*).

The C-terminal region of HA2 runs antiparallel to the N-terminal α helix, packing in the groove between α helices in the coiled coil (Figure 10*B*). Besides forming the N cap and interacting with each other, the four capping residues also make extensive contacts with ordered residues at the C terminus, residues 174–178. Thus the N- and C-terminal residues of HA2 form an extensive set of interactions that act as an N cap to terminate the central three-stranded coiled coil and fix the N- and C-terminal regions of the molecule together at one extreme end of the rodlike structure (Figure 10*B*).

This structure, like all recombinant ectodomains, is subject to the caveats that it is not yet proven to exist as a component of the complete molecule. The crystalline construct lacks both membrane-interacting regions and lipids, and neither HA1 nor carbohydrate side chains are present. There is evidence, however, for the existence of the N cap in HA derived from virus: (*a*) Aspartic acid 37 N-caps the same α helix in the neutral pH conformation of viral HA, suggesting that the terminus of this helix is a property of the sequence. (*b*) The first residue of the helix, residue 38, is also the first residue of the proteolytically resistant core of low-pH–treated viral HA. (*c*) The residues that form the N cap—Ala-35, Ala-36, and Asp-37—are conserved in all sequences of influenza A and B virus HAs, which have overall sequence identities as low as 40% (112).

The EHA2(23-185) structure (Figures 9–11) suggests that neither the fusion peptide nor the TM anchor needs to be linked to α helices to function in membrane fusion. As noted above, this appears to contrast with the situation in SV5 (114) but is consistent with the structures of the C termini of HTLV-1 and Ebola fusion glycoproteins (118, 119, 121). In TBHA2 (Figure 11*A*), which is missing the N-cap residues, the C-terminal residues that are observed, 152 of one monomer and 162 of the other two, take different paths, suggesting that before the N cap is assembled the termini can adopt energetically similar states with different structures. Membrane fusion may be accomplished either by a transient structure like TBHA2 (Figure 11*A*), in which the C-terminal segments, anchored in the viral membrane, are not yet positioned at the far end of the rod, or by the N-capped structure (Figure 11*B*).

Hemagglutinin and Membrane Curvature

Theoretical considerations of the mechanism of membrane fusion suggest that fusion of lipid vesicles involves the interaction of their membranes to form pores through which their aqueous contents can interchange. The outer leaflets of the membrane bilayers might initially fuse to produce stalk structures in which these monolayers bend with the opposite curvature to that in the initial bilayer. Subsequently, the inner monolayers are drawn into the stalk cavity, break, and fuse to complete the fusion pore (137, 138). Consistent with these proposals, the lipid

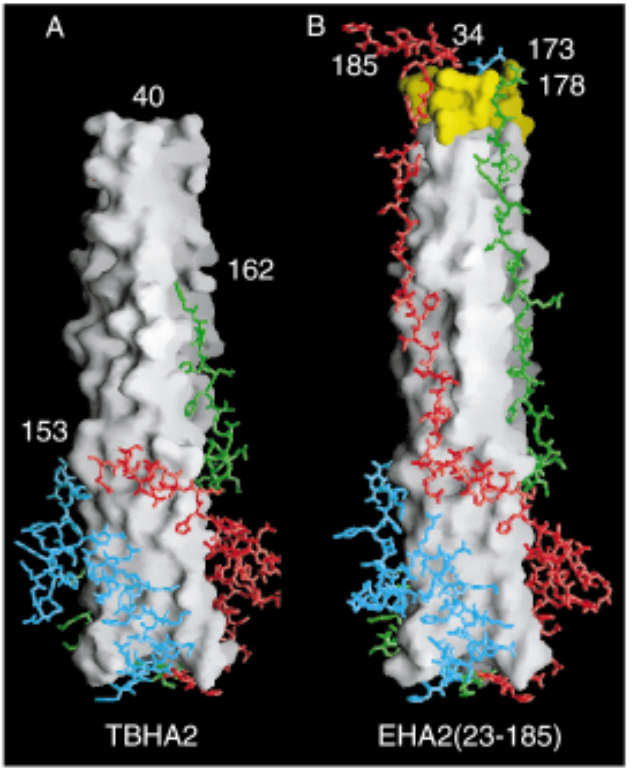

Figure 11 Comparison of TBHA2 from low-pH-treated hemagglutinin and EHA2(23–185). (*A*) TBHA2 (residues 1–27 of HA1 and 38–175 of HA2) from thermolytic digestion of low-pH-treated viral BHA. The molecular surface is the central triple-stranded coiled coil. The atomic models are the C-terminal residues beyond residue 106. The last residues visible in the electron density at the termini are labeled. (*B*) EHA2(23–185) with the N-terminal residues from 34 to 40 at the top central surface. The image is as in *A* with the visible terminal residues labeled. Figure prepared with GRASP (204).

composition of the vesicles can influence fusion (139); outer monolayers containing lipids that strongly favor the positive curvature of lipid micelles form stalks inefficiently. Incorporation of the same lipids into the inner monolayers favors pore formation. Fusion proteins including HA might influence or participate in these processes in a number of ways. The interaction of their fusion peptides with target membranes may favor the formation of stalk structures leading to hemifusion (140); a multiprotein ringlike fence may be formed around the stalk, preventing extension of hemifusion (141); or a completely proteinaceous pore may precede the formation of a lipid pore (142).

In relation to these theories, the following observations have been made on HA-mediated membrane fusion. The addition of wedge-shaped lipid molecules

such as lysophosphatidylcholine, which stabilizes positively curved monolayers to transfected cell-liposome mixtures, inhibits HA-mediated fusion (141). There have been many studies of the insertion of both synthetic and HA2-associated fusion peptides into lipids and the subsequent destabilization of the membranes (e.g. 143), but there is no consensus for how the various suggested conformations and entry angles would provide a molecular mechanism for initiating fusion. Models vary from exploiting amphipathic detergent-like qualities of fusion peptides to emphasizing anchoring functions in the formation of stress-induced lipid dimples (e.g. 144–146).

The observation that glycosylphosphatidylinositol-anchored HA molecules generate hemifusion (mixing of lipids but not vesicle contents) suggested that hemifusion may be a fusion intermediate (147–149). Subsequent experiments suggest that the glycosylphosphatidylinositol anchor might be deficient in some activity required to prevent the expansion of a hemifusion diaphragm and to proceed to fused membranes; an activity intrinsic to the structural arrangement of the HA C-terminal TM anchors (147, 149, 150).

Highly curved pits have been observed by freeze-fracture electron microscopy at sites of HA-induced fusion to lipid vesicles (151), but their relationship to the low-pH–induced HA structure is unclear. It has been suggested that the distance between the pitlike fusion sites sometimes observed in geometric rings might reflect the length of two fusion pH HAs lying horizontally between the fusing membranes (108).

Hemagglutinin and Pore Formation

Formation of a physical pore (or pores) precedes fusion between membrane-bound compartments. The earliest pore formed during HA-mediated fusion (152–157) has been observed by electrophysiological measurements to flicker, a property usually associated with channel-forming proteins but also exhibited during the fusion of protein-free lipid membranes (158). Such early flickering pores become sustained channels capable of transmitting small organic molecules (e.g. 156, 157, 159). Protein pores with such properties are often oligomeric, and indications that fusion kinetics depend on the surface density of HA trimers in lipid vesicles and on the expression level of HA in cells (147, 160, 161), as well as modeling of the kinetic events during fusion (159, 162), have led to estimates that complexes of between 3 and 6 trimers may be required, but uncertainty remains regarding the requirement and nature of these proposed higher-order complexes.

In experiments on the fusion of erythrocytes to HA-expressing cells, the expansion of an initial pore into a fusion event (141, 150, 156, 157) required HA molecules in their fusion pH conformation and depended on the density of activated molecules and the time of incubation after activation (141). The inter-HA interactions suggested by these experiments to be present during the membrane fusion event also remain uncharacterized. Rosettes of fusion pH molecules have been observed on lipid membranes by electron microscopy (98, 163), but their relevance to membrane fusion is unclear (see 163), and they cannot be distinguished

by electron microscopy from nonspecific aggregation of fusion peptides to form protein-protein micelles of the type formed by association of membrane anchors of membrane proteins.

No intertrimer interactions have been observed in crystals of fusion pH HA domains (104, 112) or any other virus fusion subunit ectodomain, but all of the molecules crystallized have lacked both the N-terminal fusion peptides and the C-terminal membrane anchors. All the crystalline fusion protein ectodomains studied have also lacked segments of the receptor-binding domain that form part of the glycoprotein stem, such as HA1 residues 1–50 and 275–328, which may have roles in fusion (164). Suggestions that residues near the reverse turn in the fusion pH HA might be involved in intertrimer contacts, made from a study of a short HA2 (residues 1–127) ectodomain fragment (165), are subject to the likelihood that such half ectodomains may have aggregation properties that differ from those of a whole, stably folded ectodomain. Similarly the shorter HA2 fragment, residue 54–93, which has been claimed to bind lipids without a fusion peptide (166), appeared not to represent the properties of longer ectodomains (96, 110).

The Coupling of Hemagglutinin Refolding Free Energy to Membrane Fusion

The free energy released by refolding and rearrangement of HA structure at fusion pH, which is reflected in the increased thermal denaturation temperature of HA in the fusion pH conformation, may be used in several steps in the process of membrane fusion. The locations of both the N-terminal fusion peptide and the C-terminal membrane anchor at one end of the newly formed rodlike structure of HA2 suggest that refolding brings the viral and cellular membranes with which they are associated into close proximity, overcoming forces that the membranes experience as they approach each other (167). Interaction of the N-terminal fusion peptide with the target endosomal membrane may additionally participate in the bending of its outer monolayer, required to form a negatively curved stalk structure (140, 168). If higher-order complexes of HA are necessary for fusion, their formation may provide additional energy, perhaps from interactions with membrane anchors, to restrict fusion to the site of complex formation (169) and to complete pore formation through the fusion of inner endosomal and inner viral-membrane monolayers; the fusion peptides themselves may act to lower the rupture tension of the transmonolayer contact that these monolayers are proposed to form (168). Knowledge of the structures of the membrane-associated regions of HA and of fusion intermediates that have been suggested by experiments at low temperature (141) would give information on these possibilities and on the mechanism of protein-mediated membrane fusion. The observations that the unfolding temperatures of the fusion conformations of other virus fusion glycoproteins are also above 90°C suggests that there may also be substantial free energies available to drive these fusion events (114).

Each of the components of HA refolding may participate in the membrane fusion mechanism and in the provision of free energy. The low-pH-induced extension

of the central triple-stranded coiled coil of HA2 exposes the fusion peptide and creates a central scaffold for assembly of the outer, antiparallel polypeptide layer. Exposure of the fusion peptide, because it is nonpolar, allows it to insert into the target cell membrane or into the viral membrane (96) or to associate with other fusion peptides to form protein-protein micelles (93). Models of fusion by each possibility have been proposed (e.g. 108, 146, 170). In vivo, receptor binding may direct fusion peptides into the target membrane (171), or those that insert into the virus membrane may lead to inactive HA, as suggested by the similarity of the structure formed and the state of the molecule after fusion, when the fusion peptides and C-terminal anchors will be in the same membrane (the fused membrane) (104, 111). Formation of the central scaffold may provide a guide for the C-terminal membrane anchors to migrate toward the fusion peptides as the outer layer of the rodlike molecule assembles (Figure 11*A* and *B*).

The refolding of helical residues 105–110 to form a reverse turn and the consequent jackknifing back of helical residues 112–129 and the β sheet packed against it (residues 130–133 and 137–140) generate a new hydrophobic core at one end of the central coiled coil in the HA (104). This may stabilize the growing coiled coil and nucleate the assembly of the outer layer, and the reversal in direction may displace the HA1 receptor-binding domain from the site of membrane fusion (Figure 7). Similar small hydrophobic cores are found at analogous positions in the retroviral TMs and Ebola GP2 (117–119, 121), but may not be necessary for outer-layer assembly, based on the observation that the residues at the chain direction reversal in HIV and SIV gp41 can be removed. As noted above, a disulfide bond, analogous to that between HA1 and HA2 at the turn end of the fusion pH rod, probably exists between GP1 and GP2 of Ebola virus (121), suggesting that transposing receptor domains away from the membrane fusion site may be a general function of the loops and domains that form the turn in these virus fusion glycoproteins.

The assembly in the outer layer of 25-residue-long extended chains (HA2 152–177) packed in the grooves between the core α helices and the formation of the N-cap clamping the N- and C-terminal regions together may provide free energy either to bring the membranes together or to stabilize them in a juxtaposed position (Figure 11*A* and *B*). The difference in melting temperatures of 10°C between soluble HA2 constructs with and without the N-cap residues suggests that some free energy is available even at this stage in the conformational change when the N cap forms (112). Whether specific refolding events releasing free energy are coupled to particular stages of fusion such as the formation of a highly curved lipid intermediate early in the fusion process or a later transition state leading to the formation of an aqueous channel requires a better understanding of the relationship between the kinetics of conformational refolding and the kinetics of the steps of lipid rearrangements.

The possibility that SNARE proteins may form α helices continuously from their ectodomains into their membrane anchors suggested that the formation of the *v*- and *t*-SNARE coiled coil and the stiffness of α helices could distort the apposed prefusion bilayers at the site of membrane attachment (124). The architecture of

HIV and SIV gp41 and F1 of SV5, which are α helical as far as their ectodomains have been visualized, suggests that they could also use such a distortion mechanism (114; Figure 8). The outer layer of the HA is clearly nonhelical (Figure 11*B*), and evidence suggests that the inner-core triple-stranded coiled coil is terminated and capped by a conserved structure that terminates the N-terminal helices as well, rendering connection to the fusion peptide susceptible to protease and presumably flexible (112). This suggests that the linkers to both the fusion peptide and the C-terminal membrane anchor are nonhelical in HA, and such a distortion mechanism is unlikely to be involved. These observations are all subject to the caveat that all of the fusion domain structures were determined in the absence of the membrane attachment segments and the remainder of the glycoprotein.

Inhibitors of Membrane Fusion

Each of the stages in the priming and activation of HA for its participation in membrane fusion presents a different target for inhibition and the development of antiviral agents. Inhibition of the cleavage of the precursor HA0, which is essential for subsequent stages of infection, has been achieved by using peptidylchloroalkylketone inhibitors of furin (172), and the serine protease, tryptase Clara, has been shown to be inhibited by two natural molecules—a mucus protease inhibitor and C-terminal fragments derived from it (173, 174) and a pulmonary surfactant (175). Prevention of insertion of the newly generated fusion peptide into the charged cavity that is adjacent to the site of HA0 cleavage, by filling it before cleavage, represents an alternative inhibition of this priming stage that remains to be explored (82). Even a reversible inhibitor binding in the cavity may cause cleaved HA to aggregate during priming and inactivate through interactions of the excluded fusion peptides. It seems likely that other virus fusion glycoprotein precursors that require cleavage to prime their fusion activity may have similar cavities that are potential inhibitor targets.

Attempts to prevent the changes in HA structure required for fusion by neutralizing the fusion pH trigger with the weak base amantadine (e.g. 88) or by directly binding small molecules to the HA to lock it in its neutral-pH form have been reported. For HA of the H3 subtype tert-butyl hydroquinone, a compound derived from a structure-based inhibitor search was shown to inhibit the fusion pH-induced changes in conformation and to block infectivity (176, 177). Diiodofluorescein blocked infectivity by prematurely facilitating the conformational change at higher pH (177). For HAs of the H1 and H2 subtypes, screens of chemical libraries coupled with molecular modeling have also revealed compounds that reversibly block the conformational changes required for fusion and infectivity (178–181). Attempts to define the sites of interaction of these compounds with HA by characterizing resistant mutants and by labeling with photoaffinity analogs of the inhibitors have also been reported (180).

By comparison with experiments on HIV, in which peptide inhibitors of infection based on predicted α-helical segments of gp41 apparently block viral entry by preventing the conformational change in gp41 required for membrane fusion

(182), analogous peptides based on HA2 structure may also block HA-mediated fusion. The HIV gp41 inhibitory peptides, which correspond to the core coiled coil segment and to the outer-layer α helix of gp41, have been proposed to act on a transient state of the molecule as it refolds to the double-layered rodlike conformation (108, 110, 116, 125, 183), and evidence for this mechanism of action has been obtained (184–188). Peptides corresponding to analogous fragments of the paramyxovirus SV5 and the retrovirus HTLV-1 membrane fusion glycoproteins also inhibit membrane fusion either completely or beyond the stage of outer monolayer fusion (189–192).

Carbobenzoxy N-terminally blocked synthetic peptide analogs of the N-terminal sequence of the fusion peptides of paramyxoviruses inhibit virus replication (193, 194) by blocking virus penetration, cell fusion, and hemolytic activities (195). The specific N-terminal sequence was essential for these effects, although peptides with an N-terminal D-amino acid were found to be most active. Similar analogs of the influenza HA fusion peptide N terminus were shown to be specific inhibitors of influenza but were less effective (196, 197). The mechanism of action of these inhibitors is not known.

THE EVOLUTION OF INFLUENZA VIRUS FUSION GLYCOPROTEINS

Influenza A viruses contain two surface glycoproteins, the HA with receptor-binding and membrane fusion activities and the NA, which is a receptor-destroying enzyme. Influenza C viruses contain a single glycoprotein, hemagglutinin esterase fusion (HEF), which has all three activities; receptor binding, membrane fusion, and an antireceptor esterase, a 9-*O*-acetylase that removes the 9-*O*-acetyl substituent from the receptor 9-*O*-acetyl-sialic acid. The structure of HEF showed that, despite only 12% sequence identity, the membrane-distal receptor-binding domains of HEF and HA (Figure 12) and the extended helix containing stems of the molecules are very similar (164, 198a). The esterase domain is extremely similar to known mammalian and bacterial esterases, and a vestigial (inactive) fragment of the domain is present in the influenza A HA. In addition the structure suggests that the receptor domain is inserted into a surface loop of the esterase and that the esterase domain is inserted into a surface loop of the stem. Both HEF and HA, therefore, may have been assembled from preformed domains (Figure 12). This possibility suggests the structure of an ancestral membrane fusion protein that contained not only HEF2 or HA2 but also the first and last $\sim$50 residues of HEF1 or HA1, that is, the whole stem of HA or HEF. It is also possible that these segments of HEF1 and HA1 (F1 and F2 in Figure 12) may have roles in membrane fusion, for example in regulating the low-pH-induced refolding or during the formation of a putative oligomeric fusion pore.

Similar modular structures of retrovirus and filovirus envelope glycoproteins are suggested by biochemical data (128, 199, 200) and by the structure of the HIV-1 gp120 fragment (201), which shows that the two ends of the receptor-binding

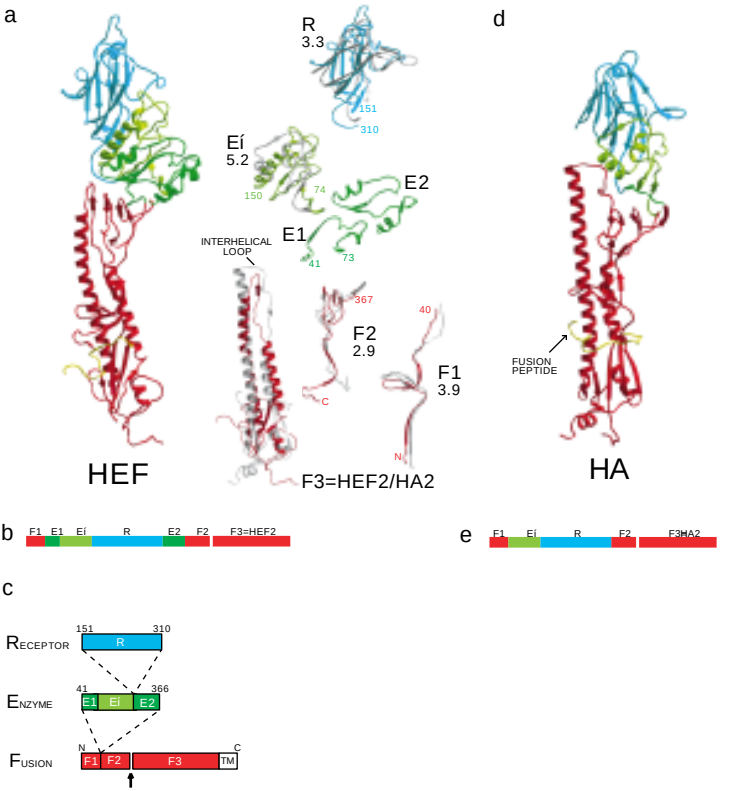

Figure 12 Comparison of HEF and HA monomers. (*a*) HEF monomer structure and exploded views of the sequence segments. Superposition of corresponding HA [X-31 strain; protein data base (PDB) code 1he] segments are shown with rms values below the segment name. (*b*) Linear order of the sequence segments in HEF, labeled by domains. (*c*) Topological relationship of the compact domains in HEF. (*d*) HA monomer structure with sequence segments labeled by domains. (*e*) Linear order of the sequence segments in HA, labeled by domain. Reprinted with permission; see Reference (164). http://www.nature.com

domain are very near at one end of the domain (like the two ends of the R domain in Figure 12), consistent with the insertion of the receptor-binding domain into a loop of a stem domain.

The F3 domains of HA and HEF are very similar in structure (Figure 12); each monomer possesses a central α helix along the threefold axis and a smaller N-terminal helix packed antiparallel on the outside and connected by an interhelical loop. In HEF2, although the central helices interact closely in the middle, like HA, they diverge from the trimer axis at both ends. At the top, the interhelical loops interpose between the first five turns of the long helices (residues 80–97) where loop residues HEF2 Arg-69 and central-helix residues HEF2 Glu-95 form

salt bridges and contact an unidentified ion (possibly a sulfate) on the trimer axis (164). Although HEF2 has a sequence deletion of seven residues in the interhelical loop region, this difference would preserve the register of the heptads during the formation of an extended triple-stranded coil in the low-pH conformation, like that in HA. Unlike HA, however, the top third of the triple-stranded helical bundle must first make interactions on the trimer axis after the removal of the interhelical loop, before the N-terminal coiled-coil extension could form.

The three (HEF2116) tryptophans interact to form the last contact on the trimer axis, below which the helices diverge as in HA (164, 198a). Unlike HA, in which residues 2 (Leu) and 3 (Phe) of the HA2 N-terminal fusion peptide interact across the trimer axis, HEF2 residues Val-11 and Leu-12 are closest to the trimer axis, but further penetration is blocked by tryptophans 116. Residues N terminal to residue 10 fold back out to the surface of the protein, where aspartic acids at positions 5 and 6 of HEF2 can interact with Arg-29 and Lys-30 of HEF2 and Lys-4 of HEF1. Lysine-9 of HEF, homologous in sequence to His-17 of HA1, is also completely buried behind the fusion peptide in cleaved HEF. It is the only buried ionizable residue in the stem of HEF. Its ε-amino group makes only two hydrogen bonds with its uncharged neighbors, indicating that it may be uncharged, with a depressed pKa. Because the structure of uncleaved, precursor HEF0 is not known, it is not known whether Lys-9 of HEF1 is on the surface of a cavity in that conformation. Residues 1–4 of HEF2 appear disordered on the surface of the molecule. In HEF the residues that are functionally analogous to the fusion peptide of HA, that is, the buried residues whose exposure would convert a soluble protein into a lipophilic one, are displaced along the sequence by six residues. HEF may therefore be regarded as having an internal fusion peptide, as proposed for a number of virus fusion proteins like Ebola GP2 and for those that do not require cleavage activation. The conformation of the N terminus of the HEF2 fusion peptide, therefore, suggests that some fusion peptides may insert into their fusion target membranes as loops.

LITERATURE CITED

1. Gottschalk A. 1959. In *The Viruses*, ed. FVM Burnet, WVM Stanley, 3:51–61. New York: Academic
2. Wiley DC, Skehel JJ. 1987. *Annu. Rev. Biochem.* 56:365–94
3. Wilson IA, Skehel JJ, Wiley DC. 1981. *Nature* 289:366–73
4. Weis W, Brown JH, Cusack S, Paulson JC, Skehel JJ, et al. 1988. *Nature* 333:426–31
5. Nobusawa E, Aoyama T, Kato H, Suzuki Y, Tateno Y, et al. 1991. *Virology* 182:475–85
6. Watowich S, Skehel JJ, Wiley DC. 1994. *Structure* 2:719–31
7. Sauter NK, Hanson JE, Glick GD, Brown JH, Crowther RL, et al. 1992. *Biochemistry* 31:9609–21
8. Eisen MB, Sabesan S, Skehel JJ, Wiley DC. 1997. *Virology* 232:19–31

9. Sauter NK, Bednarski MD, Wurzburg BA, Hanson JE, Whitesides GM, et al. 1989. *Biochemistry* 28:8388–96
10. Machytka D, Kharitonenkov I, Isecke R, Hetterich P, Brossmer R, et al. 1993. *FEBS Lett.* 334:117–20
11. Hanson JE, Sauter NK, Skehel JJ, Wiley DC. 1992. *Virology* 189:525–33
12. Kelm S, Paulson JC, Rose U, Brossmer R, Schmid W, et al. 1992. *Eur. J. Biochem.* 205:147–53
13. Martin J, Wharton SA, Lin YP, Takemoto DK, Skehel JJ, et al. 1998. *Virology* 241: 101–11
14. Sauter NK, Glick GD, Crowther RL, Park S-J, Eisen MB, et al. 1992. *Proc. Natl. Acad. Sci. USA* 89:324–28
15. Pritchett TJ, Paulson JC. 1989. *J. Biol. Chem.* 264:9850–58
16. Rogers GN, Paulson JC, Daniels RS, Skehel JJ, Wilson IA, et al. 1983. *Nature* 304:76–78
17. Rogers GN, D'Souza BL. 1989. *Virology* 173:317–22
18. Connor RJ, Kawaoka Y, Webster RG, Paulson JC. 1994. *Virology* 205:17–23
19. Gambaryan AS, Tuzikov AB, Piskarev VE, Yamnikova SS, Lvov D, et al. 1997. *Virology* 232:345–50
20. Matrosovich MN, Gambaryan AS, Teneberg S, Piskarev VE, Yamnikova SS, et al. 1997. *Virology* 233:224–34
21. Ito T, Couceiro JN, Kelm S, Baum LG, Krauss S, et al. 1998. *J. Virol.* 72:7367–73
22. Matrosovich M, Zhou N, Kawaoka Y, Webster R. 1999. *J. Virol.* 73:1146–55
23. Baum LG, Paulson JC. 1990. *Acta Histochem. Suppl.* 40:35–38
24. Couceiro JN, Paulson JC, Baum LG. 1993. *Virus Res.* 29:155–65
25. Matrosovich M, Gao P, Yoshihiro Kawaoka Y. 1998. *J. Virol.* 72:6373–80
26. Naeve CW, Hinshaw VS, Webster RG. 1984. *J. Virol.* 51:567–69
27. Vines A, Wells K, Matrosovich M, Castrucci MR, Ito T, et al. 1998. *J. Virol.* 72:7626–31
28. Hardy CT, Young SA, Webster RG, Naeve CW, Owens RJ. 1995. *Virology* 211:302–6
29. Daniels RS, Jeffries S, Yates P, Schild GC, Rogers GN, et al. 1987. *EMBO J.* 6:1459–65
30. Robertson JS, Bootman JS, Newman R, Oxford JS, Daniels RS, et al. 1987. *Virology* 160:31–37
31. Meyer WJ, Wood JM, Major D, Robertson J, Webster RG, et al. 1993. *Virology* 196:130–37
32. Ito T, Suzuki Y, Takada A, Kawamoto A, Otsuki K, et al. 1997. *J. Virol.* 71:3357–62
33. Gambaryan AS, Roberston JS, Matrosovich MN. 1999. *Virology* 258:232–39
34. Rogers GN, Daniels RS, Skehel JJ, Wiley DC, Wang XF, et al. 1985. *J. Biol. Chem.* 260:7362–67
35. Daniels RS, Douglas AR, Skehel JJ, Wiley DC, Naeve CW, et al. 1984. *Virology* 138:174–77
36. Rogers GN, Paulson JC. 1983. *Virology* 127:361–73
37. Pritchett TJ, Brossmer R, Rose U, Paulson JC. 1987. *Virology* 160:502–6
38. Takemoto DK, Skehel JJ, Wiley DC. 1996. *Virology* 217:452–58
39. Spaltenstein A, Whitesides GM. 1991. *J. Am. Chem. Soc.* 113:686–87
40. Sabesan S, Duus JO, Domaille P, Kelm S, Paulson JC. 1991. *J. Am. Chem. Soc.* 113:5865–66
41. Glick GD, Toogood PL, Wiley DC, Skehel JJ, Knowles JR. 1991. *J. Biol. Chem.* 266:23660–69
42. Reuter JD, Myc A, Hayes MM, Gan ZH, Roy R, et al. 1999. *Bioconjugate Chem.* 10:271–78
43. Bean WJ, Schell M, Katz J, Kawaoka Y, Naeve C, et al. 1992. *J. Virol.* 66:1129–38
44. Wiley DC, Wilson IA, Skehel JJ. 1981. *Nature* 289:373–78
45. Knossow M, Daniels RS, Douglas AR, Skehel JJ, Wiley DC. 1984. *Nature* 311: 678–80

46. Bizebard T, Gigant B, Rigolet P, Rasmussen B, Diat O, et al. 1995. *Nature* 376:92–94
47. Fleury D, Wharton SA, Skehel JJ, Knossow M, Bizebard T. 1998. *Nat. Struct. Biol.* 5:119–23
48. Wrigley NG, Brown EB, Daniels RS, Douglas AR, Skehel JJ, et al. 1983. *Virology* 131:308–14
49. Fleury D, Barrere B, Bizebard T, Daniels R, Skehel J, et al. 1999. *Nat. Struct. Biol.* 6:530–34
50. Colman PM, Varghese JN, Laver WG. 1983. *Nature* 303:41–47
51. Rossmann MG, Arnold E, Erickson JW, Frankenberger EA, Griffith JP, et al. 1985. *Nature* 317:145–53
52. Hogle JM, Chow M, Filman DJ. 1985. *Science* 229:1358–65
53. Wyatt R, Kwong PD, Desjardins E, Sweet RW, Robinson J, et al. 1998. *Nature* 393: 705–11
54. Caton AJ, Brownlee GG, Yewdell JW, Gerhard W. 1982. *Cell* 31:417–27
55. Daniels RS, Douglas AR, Skehel JJ, Wiley DC. 1983. *J. Gen. Virol.* 64:1657–62
56. Daniels RS, Douglas AR, Skehel JJ, Waterfield MD, Wilson IA, et al. 1983. In *The Origin of Pandemic Viruses*, ed. WG Laver, pp. 1–7. New York: Elsevier
57. Skehel JJ, Stevens DJ, Daniels RS, Douglas AR, Knossow M, et al. 1984. *Proc. Natl. Acad. Sci. USA* 81:1779–83
58. Verhoeyen M, Fang R, Jou W, Devos R, Huylebroeck D, et al. 1980. *Nature* 286:771–76
59. Volchkov VE, Blinov VM, Netesov SV. 1992. *FEBS Lett.* 305:181–84
60. Schonning K, Jansson B, Olofsson S, Hansen J. 1996. *J. Gen. Virol.* 77:753–58
61. Reitter J, Means R, Desrosiers R. 1998. *Nat. Med.* 4:679–84
62. Colman P. 1997. *Structure* 5:591–93
63. Smith TJ, Chase ES, Schmidt TJ, Olson NH, Baker TS. 1996. *Nature* 383:350–54
64. Clackson T, Wells J. 1995. *Science* 267: 383–86
65. Claas EC, Osterhaus AD, van Beek R, De Jong JC, Rimmelzwaan GF, et al. 1998. *Lancet* 351:472–77
66. Subbarao K, Klimov A, Katz J, Renuery H, Lim W, et al. 1998. *Science* 279:393–95
67. Yuen KY, Chan PKS, Peiris M, Tsang DNC, Que TL, et al. 1998. *Lancet* 351: 467–71
68. World Health Organization. 1999. *WHO Wkly. Epidemiol. Rec.* Vol. 74
69. Kawaoka Y, Yamnikova S, Chambers TM, Lvov D, Webster RG. 1990. *Virology* 179:759–67
70. Rohm C, Zhou NA, Suss JC, Mackenzie J, Webster RG. 1996. *Virology* 217:508–16
71. Gething MJ, Doms RW, York D, White J. 1986. *J. Cell Biol.* 102:11–23
72. Copeland C, Zimmer K, Wagner K, Healey G, Mellman I, et al. 1988. *Cell* 53:197–209
73. Hebert D, Foellmer B, Helenius A. 1995. *Cell* 81:425–33
74. Garten W, Klenk H. 1983. *J. Gen. Virol.* 64:2127–37
75. Kido H, Yokogoshi Y, Sakai K, Tashiro M, Kishino Y, et al. 1992. *J. Biol. Chem.* 267:13573–79
76. Bosch FX, Garten W, Klenk HD, Rott R. 1981. *Virology* 113:725–35
77. Webster RG, Rott R. 1987. *Cell* 50:665–66
78. Perdue ML, Garcia M, Senne D, Fraire M. 1997. *Virus Res.* 49:173–86
79. Stieneke-Grober A, Vey M, Angliker H, Shaw E, Thomas G, et al. 1992. *EMBO J.* 11:2407–14
80. Klenk HD, Garten W. 1994. *Trends Microbiol.* 2:39–43
81. Steinhauer DA. 1999. *Virology* 258:1–20
82. Chen J, Lee K-H, Steinhauer DA, Stevens DJ, Skehel JJ, et al. 1998. *Cell* 95:409–17
83. Klenk HD, Rott R. 1988. *Adv. Virus Res.* 34:247–81
84. Kawaoka Y, Webster RG. 1985. *Virology* 146:130–37

85. Deshpande KL, Fried VA, Ando M, Webster RG. 1987. *Proc. Natl. Acad. Sci. USA* 84:36–40
86. Horimoto T, Rivera E, Pearson J, Senne D, Krauss S, et al. 1995. *Virology* 213:223–30
87. Ohuchi M, Orlich M, Ohuchi R, Simpson BE, Garten W, et al. 1989. *Virology* 168:274–80
88. Daniels RS, Downie JC, Hay AJ, Knossow M, Skehel JJ, et al. 1985. *Cell* 40: 431–39
89. Lin YP, Wharton SA, Martin J, Skehel JJ, Wiley DC, et al. 1997. *Virology* 233:402–10
90. Huang RT, Rott R, Klenk HD. 1981. *Virology* 110:243–47
91. Maeda T, Ohnishi S. 1980. *FEBS Lett.* 122:283–87
92. White J, Matlin K, Helenius A. 1981. *J. Cell Biol.* 89:674–79
93. Skehel JJ, Bayley PM, Brown EB, Martin SR, Waterfield MD, et al. 1982. *Proc. Natl. Acad. Sci. USA* 79:968–72
94. Tsurudome M, Gluck R, Graf R, Falchetto R, Schaller U, et al. 1992. *J. Biol. Chem.* 267:20225–32
95. Weber T, Paesold G, Galli C, Mischler R, Semenza G, et al. 1994. *J. Biol. Chem.* 269:18353–58
96. Durrer P, Galli C, Hoenke S, Corti C, Gluck R, et al. 1996. *J. Biol. Chem.* 271: 13417–21
97. Ruigrok RW, Aitken A, Calder LJ, Martin SR, Skehel JJ, et al. 1988. *J. Gen. Virol.* 69:2785–95
98. Doms RW, Helenius A. 1986. *J. Virol.* 60:833–39
99. Doms RW, Gething MJ, Henneberry J, White J, Helenius A. 1986. *J. Virol.* 57: 603–13
100. Wharton SA, Skehel JJ, Wiley DC. 1986. *Virology* 149:27–35
101. Rott R, Orlich M, Klenk HD, Wang ML, Skehel JJ, et al. 1984. *EMBO J.* 3:3329–32
102. Ruigrok RWH, Martin SR, Wharton SA, Skehel JJ, Bayley PM, et al. 1986. *Virology* 155:484–97
103. Carr CM, Chaudry C, Kim PS. 1997. *Proc. Natl. Acad. Sci. USA* 94:14306–13
104. Bullough PA, Hughson FM, Skehel JJ, Wiley DC. 1994. *Nature* 371:37–43
105. Ward CW, Dopheide TA. 1980. *Aust. J. Biol. Sci.* 33:441–47
106. Chambers P, Pringle CR, Easton AJ. 1990. *J. Gen. Virol.* 71:3075–80
107. Carr CM, Kim PS. 1993. *Cell* 73:823–32
108. Weissenhorn W, Dessen A, Harrison SC, Skehel JJ, Wiley DC. 1997. *Nature* 387:426–30
108a. Hughson FM. 1997. *Curr. Biol.* 7:R565–69
109. Skehel JJ, Wiley DC. 1998. *Cell* 95:871–74
110. Chen J, Wharton SA, Weissenhorn W, Calder LJ, Hughson FM, et al. 1995. *Proc. Natl. Acad. Sci. USA* 92:12205–9
111. Wharton SA, Calder LJ, Ruigrok RWH, Skehel JJ, Steinhauer DA, et al. 1995. *EMBO J.* 14:240–46
112. Chen J, Skehel JJ, Wiley DC. 1999. *Proc. Natl. Acad. Sci. USA* 96:8967–72
113. Chen J, Skehel JJ, Wiley DC. 1998. *Biochemistry* 37:13643–49
114. Baker KA, Dutch RE, Lamb RA, Jardetzky TS. 1999 *Mol. Cell* 3:309–19
115. Caffrey M, Cai M, Kaufman J, Stahl SJ, Wingfield PT, et al. 1998. *EMBO J.* 17:4572–84
116. Chan DC, Fass D, Berger JM, Kim PS. 1997. *Cell* 89:263–73
117. Fass D, Harrison SC, Kim PS. 1996. *Nat. Struct. Biol.* 3:465–69
118. Kobe B, Center RJ, Kemp BE, Poumbourios P. 1999. *Proc. Natl. Acad. Sci. USA* 96:4319–24
118a. Hughson FM. 1997. *Curr. Biol.* 7:R565–69
119. Malashkevich VN, Schneider BJ, McNally ML, Milhollen MA, Pang JX,

et al. 1999. *Proc. Natl. Acad. Sci. USA* 96:2662–67
120. Tan KM, Liu JH, Wang JH, Shen S, Lu M. 1997. *Proc. Natl. Acad. Sci. USA* 94:12303–8
121. Weissenhorn W, Carfí A, Lee KH, Skehel JJ, Wiley DC. 1998. *Mol. Cell* 2:605–16
122. Hanson PI, Roth R, Morisaki H, Jahn R, Heuser JE. 1997. *Cell* 90:523–35
123. Poirier MA, Xiao W, Macosko JC, Chan C, Shin Y-K, et al. 1998. *Nat. Struct. Biol.* 5:765–69
124. Sutton RB, Fasshauer D, Jahn R, Brünger AT. 1998. *Nature* 395:347–53
125. Blacklow SC, Lu M, Kim PS. 1995. *Biochemistry* 34:14956–62
126. Cao J, Bergeron L, Helseth E, Thali M, Repke H, et al. 1993. *J. Virol.* 67:2747–54
127. Moore JP, Sattentau QJ, Wyatt R, Sodroski J. 1994. *J. Virol.* 68:469–84
128. Wyatt R, Desjardin E, Olshevsky U, Nixon C, Binley J, et al. 1997. *J. Virol.* 71:9722–31
129. Walker JA, Kawaoka Y. 1993. *J. Gen. Virol.* 74:311–14
130. Steinhauer DA, Wharton SA, Skehel JJ, Wiley DC. 1995. *J. Virol.* 69:6643–51
131. Qiao H, Armstrong RT, Melikyan GB, Cohen FS, White JW. 1999. *Mol. Biol. Cell* 10:2759–69
132. Orlich M, Rott R. 1994. *J. Virol.* 68:7537–39
133. Garten W, Bosch FX, Linder D, Rott R, Klenk HD. 1981. *Virology* 115:361–74
134. Gething MJ, White JM, Waterfield MD. 1978. *Proc. Natl. Acad. Sci. USA* 75: 2737–40
135. Presta LG, Rose GD. 1988. *Science* 240: 1632–41
136. Richardson JS, Richardson DC. 1988. *Science* 240:1648–52
137. Kozlov MM, Leikin SL, Chernomordik LV, Markin VS, Chizmadzhev YA. 1989. *Eur. Biophys. J.* 17:121–29
138. Siegel DP. 1993. *Biophys. J.* 65:2124–40
139. Chernomordik L, Kozlov MM, Zimmerberg J. 1995. *J. Membr. Biol.* 146:1–14
140. Colotto A, Epand RM. 1997. *Biochemistry* 36:7644–51
141. Chernomordik L, Frolov V, Leikina E, Bronk P, Zimmerberg J. 1998. *J. Cell Biol.* 140:1369–82
142. Lindau M, Almers W. 1995. *Curr. Opin. Cell Biol.* 7:509–17
143. Ishiguro R, Kimura N, Takahashi S. 1993. *Biochemistry* 32:9792–97
144. Waring AJ, Mobley PW, Gordon LM. 1998. *Proteins* 2(Suppl.):38–49
145. Macosko JC, Kim CH, Shin YK. 1997. *J. Mol. Biol.* 267:1139–48
146. Kozlov MM, Chernomordik LV. 1998. *Biophys. J.* 75:1384–96
147. Melikyan GB, White JM, Cohen FS. 1995. *J. Cell Biol.* 131:679–91
148. Kemble GW, Henis YI, White JM. 1993. *J. Cell Biol.* 122:1253–65
149. Kemble GW, Danieli T, White JM. 1994. *Cell* 76:383–91
150. Melikyan GB, Brener SA, Ok DC, Cohen FS. 1997. *J. Cell Biol.* 136:995–1005
151. Kanaseki T, Kawasaki K, Murata M, Ikeuchi Y, Ohnishi S. 1997. *J. Cell Biol.* 137:1041–56
152. Spruce AE, Iwata A, White JM, Almers W. 1989. *Nature* 342:555–58
153. Spruce AE, Iwata A, Almers W. 1991. *Proc. Natl. Acad. Sci. USA* 88:3623–27
154. Tse FW, Iwata A, Almers W. 1993. *J. Cell Biol.* 121:543–52
155. Zimmerberg J, Blumenthal R, Sarkar DP, Curran M, Morris SJ. 1994. *J. Cell Biol.* 127:1885–94
156. Melikyan GB, Niles WD, Cohen FS. 1993. *J. Gen. Physiol.* 102:1151–70
157. Melikyan GB, Niles WD, Peeples ME, Cohen FS. 1993. *J. Gen. Physiol.* 102: 1131–49
158. Chanturiya A, Chernomordik LV, Zimmerberg J. 1997. *Proc. Natl. Acad. Sci. USA* 94:14423–28

159. Blumenthal R, Sarkar DP, Durell S, Howard DE, Morris SJ. 1996. *J. Cell Biol.* 135:63–71
160. Danieli T, Pelletier SL, Henis YI, White JM. 1996. *J. Cell Biol.* 133:559–69
161. Ellens H, Bentz J, Mason D, Zhang F, White JM. 1990. *Biochemistry* 29:9697–707
162. Clague MJ, Schoch C, Blumenthal R. 1991. *J. Virol.* 65:2402–7
163. Ruigrok R, Hewat E, Wade R. 1992. *J. Gen. Virol.* 73:995–98
164. Rosenthal PB, Zhang X, Formanowski F, Fitz W, Wong C-W, et al. 1998. *Nature* 396:92–96
165. Kim CH, Macosko JC, Shin YK. 1998. *Biochemistry* 37:137–44
166. Yu YG, King DS, Shin YK. 1994. *Science* 266:274–76
167. Rand RP. 1981. *Annu. Rev. Biophys. Bioeng.* 10:277–314
168. Siegel DP, Epand RM. 1997. *Biophys. J.* 73:3089–111
169. Rand RP, Parsegian VA. 1986. *Annu. Rev. Physiol.* 48:201–12
170. Bentz J, Ellens H, Alford D. 1990. *FEBS Lett.* 276:1–5
171. Millar BMB, Calder LJ, Skehel JJ, Wiley DC. 1999. *Virology* 257:415–23
172. Garten W, Stieneke A, Shaw E, Wikstrom P, Klenk HD. 1989. *Virology* 172:25–31
173. Kido H, Beppu Y, Sakai K, Towatari T. 1997. *Biol. Chem.* 378:255–63
174. Kido H, Beppu Y, Imamura Y, Chen Y, Murakami M, et al. 1999. *Biopolymers* 51:79–86
175. Kido H, Sakai K, Kishino Y, Tashiro M. 1993. *FEBS Lett.* 322:115–19
176. Bodian DL, Yamasaki RB, Buswell RL, Stearns JF, White JM, et al. 1993. *Biochemistry* 32:2967–78
177. Hoffman LR, Kuntz ID, White JM. 1997. *J. Virol.* 71:8808–20
178. Luo G, Colonno R, Krystal M. 1996. *Virology* 226:66–76
179. Luo G, Torri A, Harte WE, Danetz S, Cianci C, et al. 1997. *J. Virol.* 71:4062–70
180. Cianci C, Yu KL, Dischino DD, Harte W, Deshpande M, et al. 1999. *J. Virol.* 73:1785–94
181. Plotch SJ, O'Hara B, Morin J, Palant O, LaRocque J, et al. 1999. *J. Virol.* 73:140–51
182. Kilby JM, Hopkins S, Venetta TM, DiMassimo B, Cloud GA, et al. 1998. *Nat. Med.* 4:1302–7
183. Lu M, Blacklow SC, Kim PS. 1995. *Nat. Struct. Biol.* 2:1075–82
184. Rimsky LT, Shugars DC, Matthews TJ. 1998. *J. Virol.* 72:986–93
185. Weng Y, Weiss CD. 1998. *J. Virol.* 72: 9676–82
186. Judice JK, Tom JY, Huang W, Wrin T, Vennari J, et al. 1997. *Proc. Natl. Acad. Sci. USA* 94:13426–30
187. Furuta RA, Wild CT, Weng Y, Weiss CD. 1998. *Nat. Struct. Biol.* 5:276–79
188. Munoz-Barroso I, Durell S, Skaaguchi K, Appella E, Blumenthal R. 1998. *J. Cell Biol.* 140:315–23
189. Rapaport D, Ovadia M, Shai Y. 1995. *EMBO J.* 14:5524–31
190. Lamb RA, Joshi SB, Dutch RE. 1999. *Mol. Membr. Biol.* 16:11–19
191. Joshi SB, Dutch RE, Lamb RA. 1998. *Virology* 248:20–34
192. Sagara Y, Inoue Y, Shiraki H, Jinno A, Hoshino H, et al. 1996. *J. Virol.* 70:1564–69
193. Miller FA, Dixon GJ, Arnett G, Dice JR, Rightsel WA, et al. 1968. *Appl. Microbiol.* 16:1489–96
194. Nicolaides E, DeWald H, Lipnik M, Westland R, Posler J. 1968. *J. Med. Chem.* 11:74–79
195. Norrby E. 1971. *Virology* 44:599–608
196. Richardson CD, Scheid A, Choppin PW. 1980. *Virology* 105:205–22
197. Richardson CD, Choppin PW. 1983. *Virology* 131:518–32

198. Zhang X, Rosenthal PB, Formanowski F, Fitz W, Wong CH, et al. 1999. *Acta Crystallogr. D* 55:945–61
198a. Deleted in proof
199. Helseth E, Olshevsky U, Furman C, Sodroski J. 1991. *J. Virol.* 65:2119–23
200. Pollard SR, Rosa MD, Rosa JJ, Wiley DC. 1992. *EMBO J.* 11:585–91
201. Kwong PD, Wyatt R, Robinson J, Sweet RW, Sodroski J, et al. 1998. *Nature* 393: 648
202. Kraulis PJ. 1991. *J. Appl. Crystallogr.* 24:946–50
203. Carson M. 1991. *J. Appl. Crystallogr.* 24:958–61
204. Nicholls A, Bharadwaj R, Honig B. 1993. *Biophys. J.* 64:A166 (Abstr.)

Annual Review of Biochemistry
Volume 69, 2000

CONTENTS